Research Square

Preprints are preliminary reports that have not undergone peer review.
They should not be considered conclusive, used to inform clinical practice,
or referenced by the media as validated information.

Integrating System-Level Impacts into Seismic Risk Assessment Reshapes Investment Priorities for More Resilient and Sustainable Cities

Chenbo Wang

chenbo.wang@ucl.ac.uk

University College London (UCL)

Alessia Campiche

University of Naples "Parthenope"

Nicola Caterino

University of Naples "Parthenope"

Carmine Galasso

University College London (UCL)

Antonio Occhiuzzi

University of Naples "Parthenope"

Article

Keywords: seismic risk assessment; urban sustainability; urban resilience; infrastructure interdependencies; disaster risk reduction

Posted Date: October 27th, 2026

DOI: https://doi.org/10.21203/rs.3.rs-11050858/v1

License: This work is licensed under a Creative Commons Attribution 4.0 International License.
Read Full License

Additional Declarations: No competing interests reported.

Integrating System-Level Impacts into Seismic Risk Assessment Reshapes Investment Priorities for More Resilient and Sustainable Cities

Chenbo Wang[a,b,*], Alessia Campiche[b], Nicola Caterino[b], Carmine Galasso[a], Antonio Occhiuzzi[b]

[a] *Department of Civil, Environmental and Geomatic Engineering, University College London (UCL), London, WC1E 6BT, United Kingdom*
[b] *Department of Engineering, University of Naples "Parthenope", Naples, 80143, Italy*

Abstract

Sustainable and resilient urban planning requires infrastructure investments that increase the capacity to maintain and recover essential services following disasters, yet regional seismic-risk assessments typically prioritise physical damage or direct economic loss, providing limited guidance on allocating scarce mitigation resources. Here we develop an integrated framework that quantifies a wide array of societal impact metrics across interdependent housing, transport, education and healthcare systems and identifies the least-effort mitigation strategies for attaining prescribed levels of impact reduction. Each metric is evaluated through two complementary aggregation lenses: total impacts, capturing system-wide disruption, and mean impacts, capturing the average burden borne by individual assets or users. Applying the framework to nearly 200,000 candidate mitigation strategies spanning residential buildings, bridges, schools and hospitals in Avellino, Southern Italy, under representative moment magnitude 5.0 and 6.9 earthquake scenarios, we find that residential retrofitting dominates the preferred strategy up to moderate mitigation targets, after which bridge retrofitting becomes the principal source of further impact reduction. Crucially, the value of bridge retrofitting arises less from avoided bridge damage than from preserving the road connectivity on which hospital access depends—a societal benefit invisible to damage-oriented assessments. This prioritisation remains stable across both aggregation lenses, with only the transition thresholds shifting. By linking infrastructure vulnerability, system-level societal impacts and risk-informed policy design, the framework provides a practical decision-support tool for directing resource-efficient infrastructure investment towards safer, more resilient and sustainable cities.

Keywords: seismic risk assessment; urban sustainability; urban resilience; infrastructure interdependencies; disaster risk reduction;

*Corresponding author
Email address: chenbo.wang@ucl.ac.uk (Chenbo Wang)

Introduction

The long-term resilience and sustainability of cities depend on their capacity to provide essential services, safeguard societal well-being and manage limited economic and environmental resources, including when exposed to major shocks[1–3]. Devastating natural hazards such as earthquakes threaten this capacity by damaging interconnected built and natural systems and disrupting the services and functions on which society depends[4–7]. Their consequences include extensive physical damage to the built environment and degradation of the natural environment, including the destruction of vegetation, natural habitats and biodiversity[8]; environmental burdens, such as increases in embodied carbon from the repair and replacement of damaged assets[9]; direct[10] and indirect[11,12] economic losses; casualties[13]; population displacement[14,15]; employment losses[16]; and disruption to essential services and functions related to utilities[17,18], housing[19], healthcare[20] and education[21,22].

Historic earthquakes illustrate the breadth and interdependency of these consequences. In the 2015 Gorkha earthquake sequence in Nepal, the M_w 7.8 mainshock and its aftershocks damaged approximately one million buildings, including the destruction of 600,000 residences[23], killed more than 8,600 people, injured more than 22,000 and displaced 2.6 million[24], leaving approximately 2.8 million people in need of immediate humanitarian assistance[25]. The disruption extended far beyond these direct losses: more than 20,000 coseismic landslides severed road access across fourteen districts, isolating communities, cutting major district hospitals off from medical supplies and delaying emergency response and medical relief[26–28]. Similarly, the 2009 M_w 6.3 L'Aquila earthquake in central Italy struck a building stock composed primarily of unreinforced masonry and non-ductile reinforced concrete, both highly vulnerable to ground shaking[29–31]. More than 15,000 buildings were severely damaged or collapsed, causing over 300 deaths, approximately 1,500 injuries and the displacement or homelessness of more than 70,000 people[32]. Widespread damage to 616 school buildings[33] meant that over 17,000 students could resume classes only after interventions such as the deployment of temporary modular school structures[34]. Spanning the Global South and the Global North, these cases indicate that such cascades are not confined to a particular development context.

Rising physical vulnerability—often driven by ageing and inadequately maintained infrastructure due to costs and limited resources—increases earthquake disaster risk globally. Urgent mitigation is therefore needed to improve the physical and functional safety of infrastructure and strengthen the resilience of urban systems—i.e., the capacity to maintain and recover essential functions following earthquakes. Effective strategies, including seismic retrofitting of vulnerable assets (e.g., buildings, bridges) and risk-informed urban planning[35,36], are central to the 2015–2030 Sendai Framework for Disaster Risk Reduction (DRR)[37] and Sustainable Development Goals (SDGs)[38], particularly SDG 9 on resilient infrastructure and SDG 11 on sustainable and resilient cities[39]. Designing and implementing them, however, requires quantitative evidence on earthquake impacts and on the effectiveness of interventions[40–42].

Such evidence remains narrow. Despite substantial progress in seismic risk modelling, state-of-the-art and state-of-practice regional risk assessments still focus on a limited set of impact metrics[43,44], typically direct economic losses or physical damage to buildings and infrastructure[4,5]. These metrics matter, but they provide insufficient information for disaster risk management (DRM) decisions, which require cross-sectoral coordination[43]. Earthquakes

trigger cascading, system-level impacts such as essential-service outages and population displacement[6,45–47]: damage to bridges, for instance, can disrupt the road network and in turn cut people off from healthcare services[48]. By overlooking these interlinked consequences, conventional risk assessments may undervalue interventions whose benefits arise through other systems and may therefore misdirect investments intended to support long-term urban resilience and sustainability. Even where broader societal impacts are quantified, systemic approaches are lacking for comparing how alternative allocations of mitigation resources across infrastructure sectors affect both system-wide disruption and the average burden borne by individual assets or users[49]. Many studies have evaluated engineering measures such as building retrofitting and code enforcement[14,40,50,51], but few resolve this distinction at regional scales. Policymakers are consequently left without evidence on which investment pathways deliver progressively higher levels of risk reduction with the least resources.

Here we develop an integrated, system-level framework for evaluating regional earthquake risk through the performance of interconnected infrastructure assets and the consequences of their disruptions for people. Building on Wang et al.[52], the framework introduces two key extensions. First, it broadens the assessment beyond direct structural damage to quantify consequences arising across infrastructure systems, including population displacement, temporary shelter demand, disruption to education and reduced access to healthcare. Second, it evaluates mitigation strategies through complementary representations of aggregate and mean impacts, thereby distinguishing the overall burden from the average burden experienced by individual assets or users. Together, these metrics capture both the physical and functional performance of infrastructure and the continuity and recovery of the functions it supports. By tracing how asset-level interventions propagate across infrastructure systems and population groups, the framework supports risk-informed, evidence-based prioritisation of mitigation investments that balance benefits and feasibility.

We apply the framework to the province of Avellino, Italy, under representative M_w 5.0 and M_w 6.9 earthquake scenarios. The analysis considers residential buildings, schools, hospitals, and bridges, and examines mitigation strategies based on upgrading these assets to higher seismic design standards, revealing the trade-offs between reducing impacts on people, addressing their uneven distribution and limiting investment costs. For clarity and tractability, we demonstrate the framework through hard structural strengthening, although it is readily extensible to soft policies. Avellino combines a well-documented history of high-impact events, notably the 1980 Irpinia earthquake[53], with features that make the findings broadly transferable. Its compact historic core, mixed masonry and older reinforced concrete building stock, and expanding peri-urban infrastructure[54,55] are typical of small- to medium-sized Mediterranean towns, so its hazard and vulnerability profile is representative of many southern European settings; its prevalent unreinforced masonry and pre-code reinforced concrete structures offer clear scope to test retrofit and risk-reduction strategies[56]; and extensive social, economic and governance records, alongside rich seismological and damage datasets, support high-resolution integrated analysis and modelling of hazard–damage–societal impact pathways.

The Proposed Framework

The proposed framework (Figure 1) comprises five modules—(1) Mitigation Strategies; (2) Exposure Modelling; (3) Seismic Hazard; (4) Physical Infrastructure Impact; and (5) Societal Impact—together with a Decision-making module. Modules (1) and (2) define the Urban Layout component, which describes a specific urban-planning scenario: the locations of exposed assets and the implemented mitigation measures, which may involve planned modifications to the exposure and the physical vulnerability of those assets. The Computational Modelling component, comprising modules (3)–(5), uses this information to evaluate seismic hazard, physical infrastructure impacts and the societal impacts that follow. The resulting impact metrics then inform the Decision-making module, which identifies the least-effort mitigation strategy attaining any prescribed level of impact reduction.

Mitigation Strategies

The Mitigation Strategies module defines the candidate interventions whose benefits the framework evaluates. Mitigation strategies are instruments of DRM—the application of DRR policies and strategies—which the United Nations Office for Disaster Risk Reduction (UNDRR) groups into three categories[57]: prospective DRM, which avoids the creation of new risk, for example through risk-sensitive urban planning and disaster-resilient infrastructure design[58,59]; corrective DRM, which reduces risk already present, for example by upgrading or retrofitting vulnerable assets such as buildings or bridges to higher structural standards or building codes[40]; and compensatory DRM, which strengthens the social and economic resilience of individuals and societies against residual risk, i.e., those "that remains in unmanaged form, even when effective DRR measures are in place"[60], through financial and social protection instruments such as national emergency funds, disaster relief funds, and catastrophe insurance. These interventions are also described as 'soft' (e.g., post-earthquake livelihood assistance funds) or 'hard' (e.g., physical strengthening of infrastructure) measures.

The framework accommodates all three categories. Here we illustrate it using hard corrective measures—upgrading physical infrastructure assets to higher seismic design standards, the worked example of corrective DRM in the UNDRR terminology[61]—while still evaluating them from a system-level perspective and across a broad set of societal impact metrics. This suits the Italian context of the case study, where insurance penetration for residential and public buildings remains low and non-mandatory for many asset classes, while physical retrofitting is heavily incentivised through national schemes such as the *Sismabonus*[62]. Strengthening existing assets is therefore among the most realistic and policy-relevant mitigation pathways available in Italy, and in other regions with low earthquake insurance penetration, such as Japan[63] and California, USA[64].

More specifically, a mitigation strategy is defined as the upgrading or retrofitting of certain proportions of existing infrastructure assets to the highest available seismic design standard across a geographic region of interest (e.g., a province or municipality). Let $r_{t,p} \in [0,1]$ denote the proportion of upgraded assets, hereafter the upgrading ratio, where $t = 1, \ldots, n_t$ indexes the infrastructure typology and $p = 1, \ldots, n_p$ the mitigation strategy. Only eligible assets—those not already built to the highest design code level—are considered for upgrading. For example, strategy #3 may specify that 50% ($r_{1,3}$) of residential buildings ($t = 1$), 20%

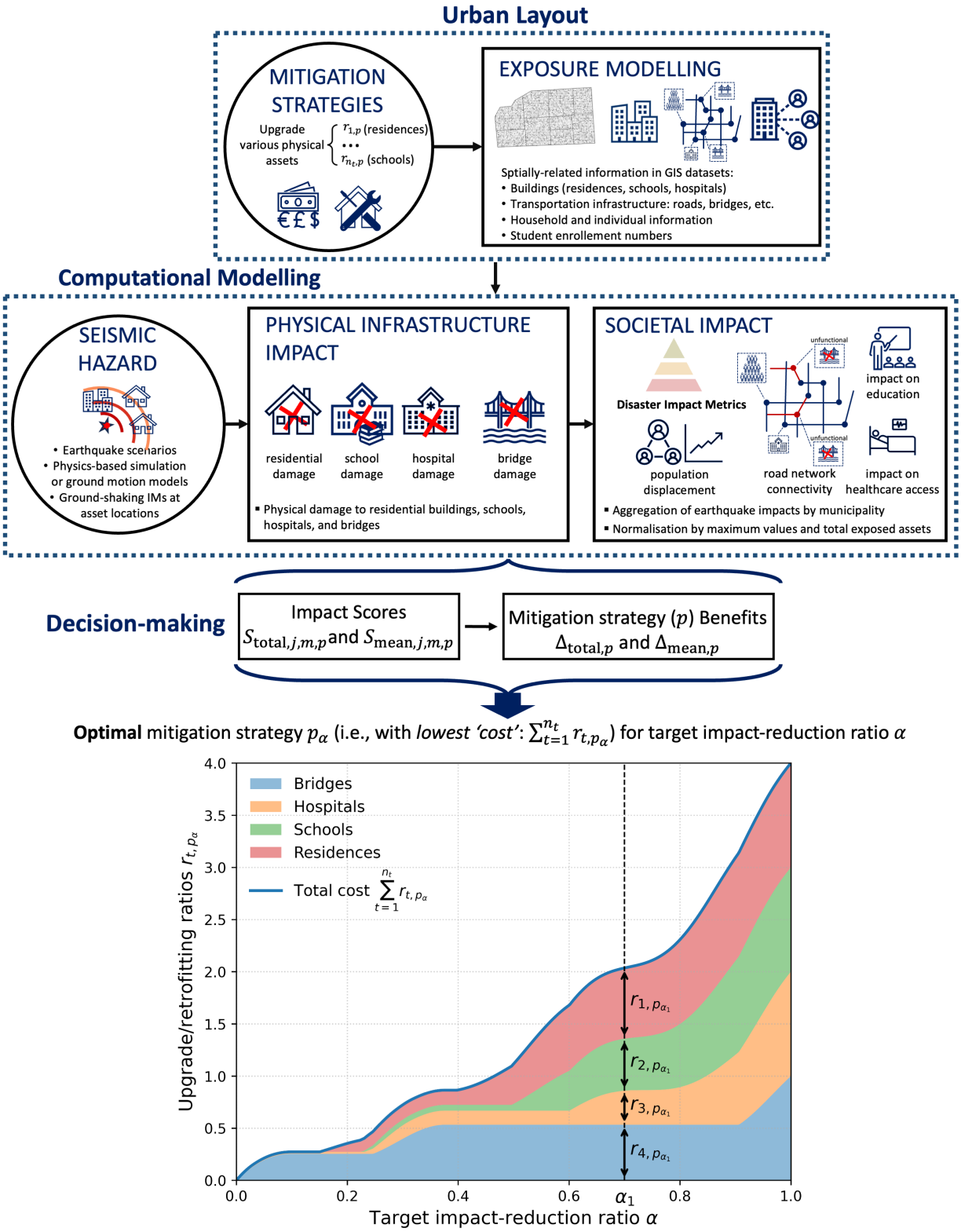

Figure 1: The proposed framework for facilitating the design of mitigation strategies that reduce the overall societal consequences of earthquakes through the strengthening of physical assets of the built environment, adapted from Wang et al.[52]. The illustrative decision-making curves show the optimal upgrading ratios, r_{t,p_α}, as functions of the target impact-reduction ratio, α, for each infrastructure typology t. The curves are stacked so that their envelope, $\sum_{t=1}^{n_t} r_{t,p_\alpha}$, is a proxy for the total implementation cost of each strategy.

($r_{2,3}$) of school buildings ($t = 2$), 75% ($r_{3,3}$) of bridges ($t = 3$) and 25% ($r_{4,3}$) of hospital buildings ($t = 4$) are upgraded to the highest seismic design code within all geographic units of the region of interest.

In practice, upgrading ratios may reflect available financial resources, explicit prioritisation criteria, or stakeholder preferences elicited through multi-criteria decision-making methods such as the analytic hierarchy process[65] or swing weighting[66]; different stakeholder groups (e.g., emergency response agencies, infrastructure operators, community representatives) may prioritise asset classes differently[4], yielding distinct sets of feasible ratios. Here we instead explore the full space of $r_{t,p}$ combinations, so that priorities emerge from the impact modelling rather than from prior stakeholder weighting. In application, their specification would ideally be informed by extensive stakeholder engagement, ensuring that the resulting portfolios reflect local priorities, resource constraints and distributional considerations.

Exposure Modelling

The Exposure Modelling module provides a spatial representation of the physical and social systems within the region of interest, characterising the assets, networks (e.g., transportation infrastructure) and populations that may be affected by an earthquake. It includes information on built assets (e.g., residences, hospitals, schools and bridges) and on the associated groups of people (e.g., households, students) exposed to potential seismic hazards. Such information may include the locations and physical vulnerability characteristics of exposed infrastructure assets (e.g., height, material of the lateral load-resisting system, construction era[67]), and the underlying population data of households and individuals.

Seismic Hazard

The Seismic Hazard module characterises the earthquake events considered and estimates the resulting ground-shaking intensity at the locations of exposed assets (e.g., buildings and bridges). It includes information on the seismic source and rupture characteristics for a prescribed catalogue of earthquake events (or scenarios). The resulting ground shaking is expressed in terms of intensity measures (IMs).

These IMs may be estimated using either physics-based simulations or empirical ground-motion models (GMMs). Physics-based simulations use dynamic or kinematic rupture models to represent the earthquake source and solve the wave-propagation equations to generate ground-motion time series at the Earth's surface[68]. Alternatively, empirical GMMs estimate the probability distribution of an IM at a site for an earthquake of a given magnitude and location, based on statistical regression analysis of ground-motion records from past earthquakes[69].

Physical Infrastructure Impact

The Physical Infrastructure Impact module translates the ground-shaking IMs into physical damage to built assets, using fragility models. Damage is represented in terms of discrete damage states (DSs) that describe increasing levels of structural or functional damage, delimited by the corresponding limit states. Fragility models—which give the probability of reaching or exceeding a given DS conditional on a specified hazard IM—can be selected

from existing model libraries on the basis of the physical vulnerability characteristics of the infrastructure, its geographic context, and other user-specific modelling requirements, such as the ability to capture particular damage mechanisms[67]. Alternatively, they may be derived specifically for the exposed assets using analytical or empirical approaches[70].

Societal Impact

The Societal Impact module combines DS calculations with additional analytical tools—such as transportation network analysis (e.g., optimal path identification using Dijkstra's algorithm[71]) and damage-to-impact or consequence models, which translate discrete DSs into societal consequences such as repair costs, casualties or service disruption[67,72,73]—to estimate a wide range of disaster impact metrics (DIMs). Alternatively, vulnerability models—giving the probability distribution of an impact conditional on the same IM[67]—translate IM values into DIMs directly. DIMs are key outputs of risk assessments and offer a tangible, policy-relevant means of communicating earthquake consequences[4]; examples include residential building recovery times, household displacement durations and educational downtime experienced by students. They may be computed for individual assets or asset typologies, aggregated to any desired geographic unit (e.g., a municipality) and, where relevant, disaggregated by socioeconomic characteristics of the affected populations, such as household income, age or gender[43], enabling both high-resolution analysis of impacts on specific population groups and system-level assessment across larger areas.

Two complementary formulations of each DIM are computed for every geographic unit: (1) the total impact, $D_{\text{total},i,j,m,p}$, representing the aggregate value of DIM i in geographic unit j for earthquake scenario m under mitigation strategy p; and (2) the mean impact, $D_{\text{mean},i,j,m,p}$, representing the corresponding average impact experienced per exposed asset or user. $D_{\text{total},i,j,m,p}$ is first estimated for each DIM, then normalised by the number of exposed assets or population associated with DIM i in geographic unit j, denoted $n_{\text{asset},i,j}$, to obtain the mean impact:

$$D_{\text{mean},i,j,m,p} = \frac{D_{\text{total},i,j,m,p}}{n_{\text{asset},i,j}} \tag{1}$$

Evaluating both is essential for meaningful comparison across infrastructure typologies, population groups and mitigation strategies: total impacts capture system-wide consequences and are therefore dominated by large, densely exposed units, whereas mean impacts capture the distributional, per-asset burden borne by an individual asset, household or user, and are insensitive to the size of the exposed portfolio.

Decision Making

The Decision-making module converts $D_{\text{total},i,j,m,p}$ and $D_{\text{mean},i,j,m,p}$ into two impact scores for each geographic unit, earthquake scenario and mitigation strategy—the total impact score $S_{\text{total},j,m,p} \in [0,1]$ and the mean impact score $S_{\text{mean},j,m,p} \in [0,1]$—supporting decisions aimed at reducing aggregate and distributional impacts, respectively. The total impact score is computed as:

$$S_{\text{total},j,m,p} = \sum_{i=1}^{n_i} w_i \times \frac{D_{\text{total},i,j,m,p}}{\max\left(D_{\text{total},i,1,1,o}, \ldots, D_{\text{total},i,n_j,n_m,o}\right)} \tag{2}$$

where n_i is the number of DIMs considered, n_j the number of geographic units in the region of interest and n_m the number of earthquake scenarios. The denominator is the maximum value of $D_{\text{total},i,j,m,p}$ across all geographic units and earthquake scenarios under the current (unmitigated) urban layout o; normalising every strategy against this common baseline keeps the resulting scores comparable across strategies. The parameter w_i denotes the relative importance weight assigned to the ith DIM, such that:

$$\sum_{i=1}^{n_i} w_i = 1 \tag{3}$$

The mean impact score is defined analogously, with D_{mean} replacing D_{total} throughout:

$$S_{\text{mean},j,m,p} = \sum_{i=1}^{n_i} w_i \times \frac{D_{\text{mean},i,j,m,p}}{\max\left(D_{\text{mean},i,1,1,o}, \ldots, D_{\text{mean},i,n_j,n_m,o}\right)} \tag{4}$$

The total and mean benefits associated with each mitigation strategy are defined as the reduction in impact scores relative to the unmitigated urban layout o, aggregated across all considered earthquake scenarios ($m = 1, \ldots, n_m$) and geographic units ($j = 1, \ldots, n_j$):

$$\Delta_{\text{total},p} = \sum_{m=1}^{n_m} \sum_{j=1}^{n_j} S_{\text{total},j,m,o} - \sum_{m=1}^{n_m} \sum_{j=1}^{n_j} S_{\text{total},j,m,p} \tag{5}$$

$$\Delta_{\text{mean},p} = \sum_{m=1}^{n_m} \sum_{j=1}^{n_j} S_{\text{mean},j,m,o} - \sum_{m=1}^{n_m} \sum_{j=1}^{n_j} S_{\text{mean},j,m,p} \tag{6}$$

To support mitigation strategy optimisation, we define a target impact-reduction ratio $\alpha \in [0, 1]$, representing the desired fraction of the maximum achievable reduction in earthquake impacts, where the maximum corresponds to upgrading all eligible infrastructure assets to the highest available seismic standard (i.e., $r_{t,p} = 1$ for all t). The value of α reflects decision makers' objectives, priorities and resource constraints in real-life decision-making processes[74], thereby specifying the level of impact reduction a mitigation strategy is intended to achieve. It may be defined using either $\Delta_{\text{total},p}$ or $\Delta_{\text{mean},p}$, according to whether risk is evaluated from an aggregate or a per-asset perspective.

For each value of α, the optimal strategy p_α is the strategy that achieves at least the target impact-reduction level while minimising the total effort/cost of upgrading:

$$\min_{p} \sum_{t=1}^{n_t} r_{t,p} \quad \text{subject to} \quad \Delta_p \geq \alpha\, \Delta_{\max} \tag{7}$$

where $r_{t,p}$ denotes the proportion of infrastructure assets of type t upgraded under strategy p, n_t is the number of infrastructure typologies considered, and $\Delta_{\max}$ is the benefit obtained when all eligible assets are upgraded. For simplicity, the sum of upgrading ratios across all

infrastructure typologies is used as a proxy for the total implementation cost, assuming that the cost of upgrading a given fraction of assets is comparable across infrastructure types. If more detailed cost information is available, the objective in Equation 7 can be readily replaced by a more realistic cost function that accounts for differences in asset-specific retrofit costs[75].

In practice, the framework is evaluated for a set of candidate strategies defined by $r_{t,p}$, each iteration producing the impact calculations for one strategy. Values of α are then sampled between 0 and 1 (e.g., $0, 0.05, 0.10, \ldots, 1.00$) and, for each, the strategy p_α meeting the target with the lowest upgrading effort is identified. Plotting r_{t,p_α} against α for each typology t and stacking the curves yields the decision-making curves (Figure 1 gives an illustrative example with $n_t = 4$: residential buildings, schools, bridges and hospitals). The shaded areas represent the upgrading effort/cost allocated to each sector, revealing how sector-specific interventions collectively achieve the prescribed target most cost-efficiently, and how the optimal allocation varies as mitigation ambition increases.

Results

The province of Avellino is located in the Campania region of southern Italy (see the bottom panels of Figure 2), one of the most seismically active regions in the Mediterranean[76].

Societal impacts

We consider six DIMs for Avellino Province, each characterised using total- and mean-impact formulations (see Table 1). The DIMs are characterised following the hierarchical structure of societal dependencies presented in Wang et al.[4], in which disaster consequences are conceptualised as emerging through interactions between physical infrastructure systems, the services they support, and the populations that depend on them. Within this framework, physical infrastructure components such as buildings, transportation infrastructure, utilities, and healthcare facilities form the foundation of the built environment, while higher-level social impacts arise from disruptions to the services and functions supported by these systems. This hierarchical representation helps emphasise how physical damage propagates into wider system-level societal impacts, thereby facilitating a more systematic interpretation of disaster consequences across interconnected urban systems. It also provides a transparent structure for communicating the relevance of different DIMs to stakeholders with varying priorities.

Each DIM is associated with the physical or social infrastructure component most directly linked to the corresponding disaster consequence. For example, the recovery time for residential buildings (DIM #1) is associated with the "building" component because it directly reflects the post-disaster functionality and repair process of the residential building stock. In contrast, the sheltering-related DIMs (DIMs #3 and #4) represent broader societal consequences arising from housing disruption, namely the immediate and longer-term displacement of affected populations. Similarly, bridge damage (DIM #2) is linked to the transportation component because bridge functionality influences mobility and connectivity across the road network, while education- and healthcare-related DIMs (#5 and #6) capture disruptions to essential services that communities rely on during both emergency response and longer-term

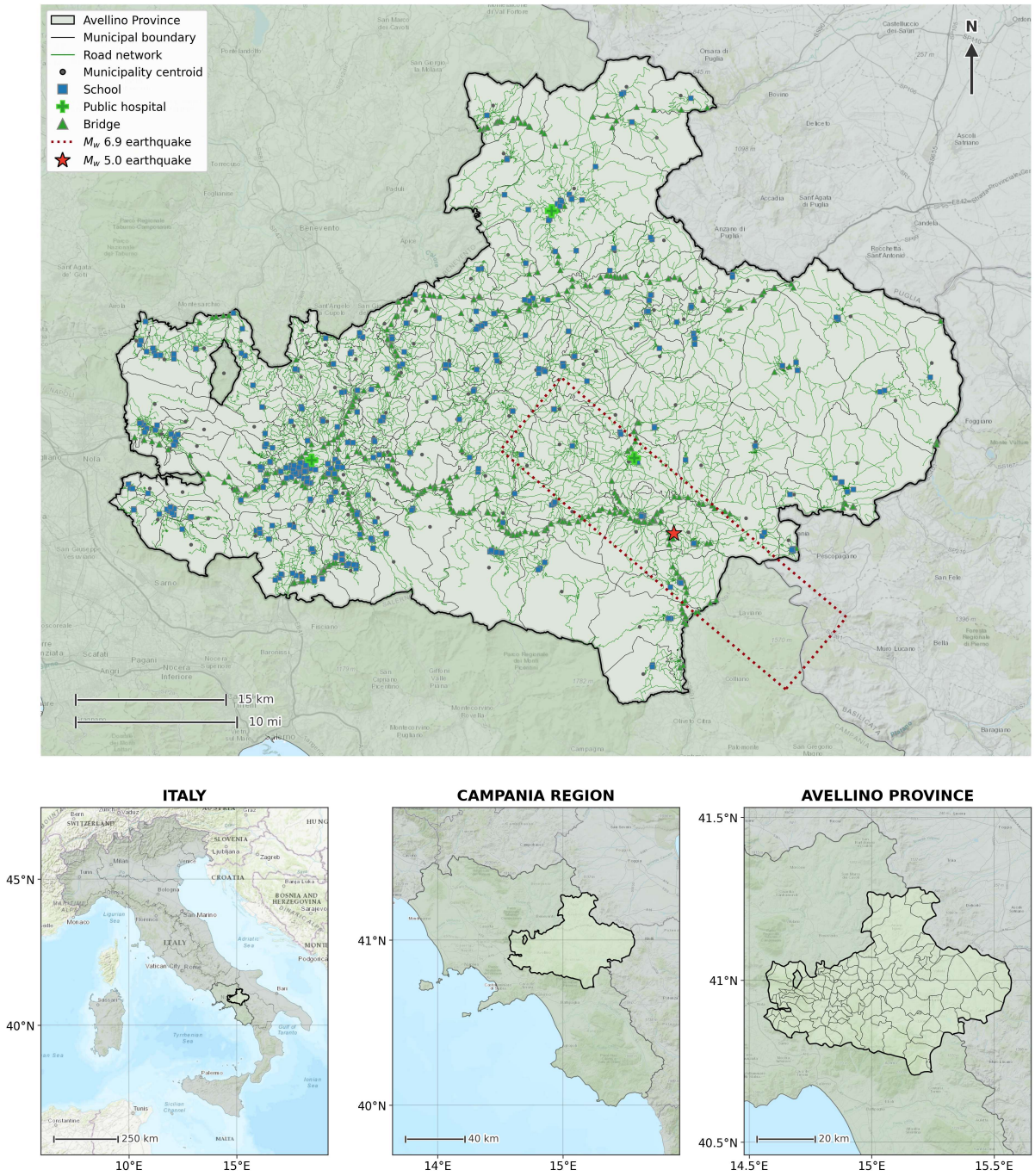

Figure 2: Study region and exposure. Top: municipalities, road network and individually geolocated assets of Avellino province—schools, public hospitals and bridges—together with the surface projection of the M_w 6.9 finite-fault rupture and the M_w 5.0 point source. Municipality centroids mark the residential and population exposure aggregation points. Bottom, left to right: location of Avellino province within Italy, within the Campania region, and its 118 municipalities.

Table 1: Total and mean DIMs considered for Avellino province.

Physical / social infrastructure	**Total impacts**	**Mean impacts**
Building	(1) Total recovery time for all residential buildings [residential buildings × days]	(1) Mean recovery time for residential buildings [days]
Transportation	(2) Total number of bridges damaged (i.e., mean DS≥ 1) [bridges]	(2) Percentage of bridges damaged [%]
Sheltering	(3) Peak population requiring immediate shelter assistance in the first month [persons] (4) Population facing protracted displacement (i.e., persistent shelter needs six months later) [persons]	(3) Percentage of population requiring sheltering in the first month [%] (4) Percentage of population facing protracted displacement [%]
Educational services	(5) Students losing access to in-person education [persons]	(5) Percentage of students losing access to in-person education [%]
Healthcare services	(6) Total drop in healthcare accessibility × population (≥ 0) [beds]	(6) Drop in municipality-level healthcare accessibility [beds/person]

recovery phases. We assign equal weights to the six DIMs (i.e., $w_i = 1/6$), in the absence of empirically elicited stakeholder preferences.

Figure 3 presents municipality-level residential recovery time (DIM #1) for the M_w 5.0 and M_w 6.9 earthquake scenarios (panels a,b), together with the total and mean loss of access to in-person education (DIM #5) for the M_w 6.9 scenario (panels c,d), under the current urban layout with no mitigation strategies applied. The same baseline configuration is used for the results shown in Figures 4 and 5. All results are averaged across the ground-motion and corresponding impact realisations.

For DIM #1, the M_w 5.0 scenario produces the largest total recovery burdens in municipalities near the hypocentre (Figure 3a), whereas the M_w 6.9 scenario results in widespread impacts across the province (Figure 3b). Some municipalities located farther from the rupture (e.g., more than 50 km away) nevertheless experience large total recovery times. The spatial patterns of DIMs #3 and #4 broadly resemble those of DIM #1 because both peak and protracted displacement strongly correlate with residential building damage. Across the municipalities, peak displacement reaches approximately 1,400 people, while protracted displacement reaches approximately 175 people; these results are not shown for brevity. For DIM #5 under the M_w 6.9 scenario, the municipalities experiencing the largest absolute numbers of affected students (Figure 3c) differ in some cases from those experiencing the largest proportional losses (Figure 3d). In the most severely affected municipalities, more than 1,000 students, or nearly 100% of enrolled students, lose access to in-person education. These municipalities are not necessarily those closest to the rupture or exposed to the strongest ground shaking, because the impacts also depend on the vulnerability of school buildings and the number of students they serve. Together, these results demonstrate that the spatial

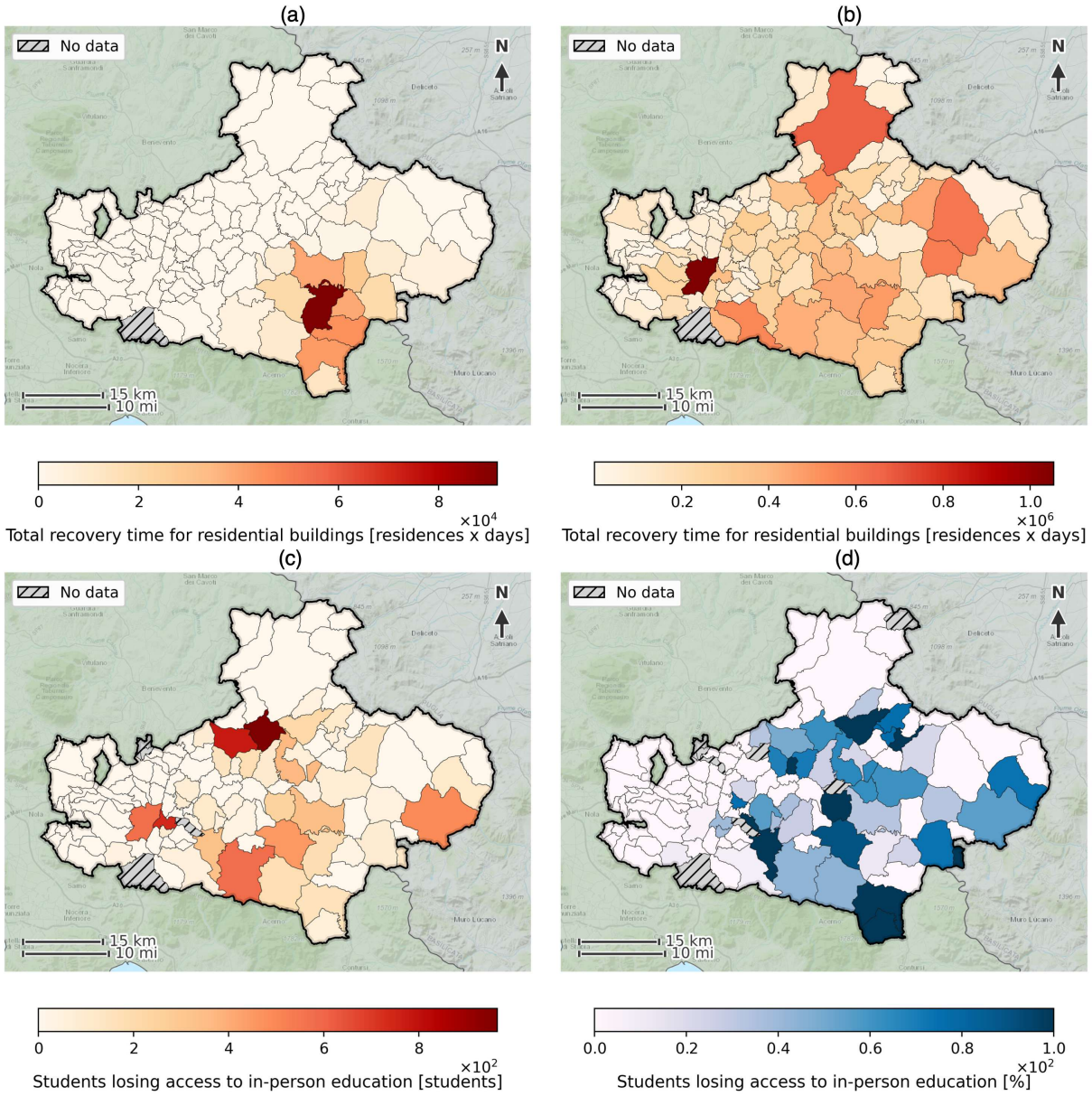

Figure 3: Municipality-level societal impacts related to residential (DIM #1) and school buildings (DIM #5) under the current urban layout with no mitigation strategies applied. (**a**, **b**) Total recovery time for residential buildings following the M_w 5.0 and M_w 6.9 earthquake scenarios, respectively. (**c**, **d**) Number and percentage of students losing access to in-person education, respectively, following the M_w 6.9 earthquake scenario. Different colour-bar ranges are used in panels **a** and **b** to reveal spatial variation within each scenario.

distribution of societal impacts cannot be inferred from hazard intensity alone, but emerges from the interaction among hazard, infrastructure vulnerability, and physical asset and population exposure.

Figure 4 presents the bridge inventory and road network of Avellino Province for the M_w 6.9 earthquake scenario under the current urban layout. It identifies the bridges and hospitals that become non-functional and the road segments that become disconnected as a result of bridge failures. Figure 5 presents the corresponding municipality-level results for bridge damage (DIM #2) and reduction in healthcare accessibility (DIM #6). Panels a,b of Figure 5 show the number of damaged bridges and the population-weighted reduction in healthcare accessibility, respectively, whereas panels c,d show the corresponding percentage of bridges damaged and mean (i.e., per person) reduction in healthcare accessibility. The spatial patterns of bridge damage and healthcare accessibility loss differ substantially. Municipalities experiencing the greatest cumulative or mean bridge damage (panels a,c of Figure 5) are not necessarily those experiencing the largest impacts on healthcare accessibility (panels b,d of Figure 5). Indeed, municipalities with no bridges—and therefore no directly attributed bridge damage—may still experience accessibility losses because of the interconnected nature of the road and healthcare systems. Such impacts may arise from the loss of feasible travel routes caused by bridge failures elsewhere, damage to hospitals serving multiple municipalities, or changes in competition for the remaining hospital capacity across the province.

The total- and mean-impact formulations also reveal different dimensions of the resulting societal burden. Municipalities with the largest mean reductions in healthcare accessibility (Figure 5d) are not necessarily those with the largest population-weighted impacts (Figure 5b). A municipality may experience a severe average reduction in accessibility but affect relatively few people, whereas a more moderate reduction in a highly populated municipality may produce a substantially greater aggregate impact. Together, these results demonstrate that cascading societal consequences cannot be inferred from the damage information of individual assets or municipalities in isolation, but require a system-level representation of the spatial and functional interdependencies among infrastructure, services, and the populations that depend on them.

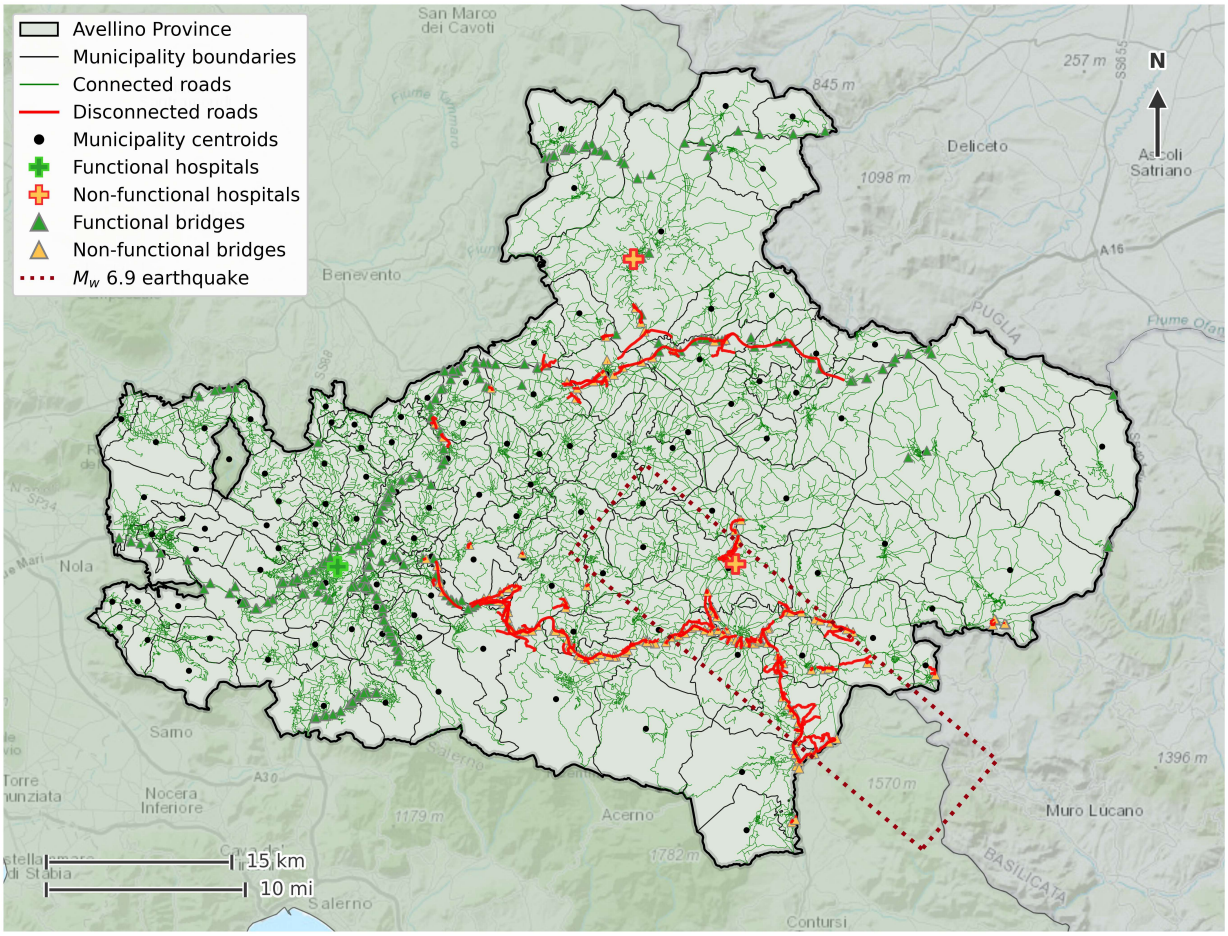

Figure 4: Bridge and hospital functionality and the resulting road-network connectivity following the M_w 6.9 earthquake scenario under the current urban layout. The figure identifies bridges and hospitals that remain functional or become non-functional, together with road segments that remain connected or become disconnected as a result of bridge failures.

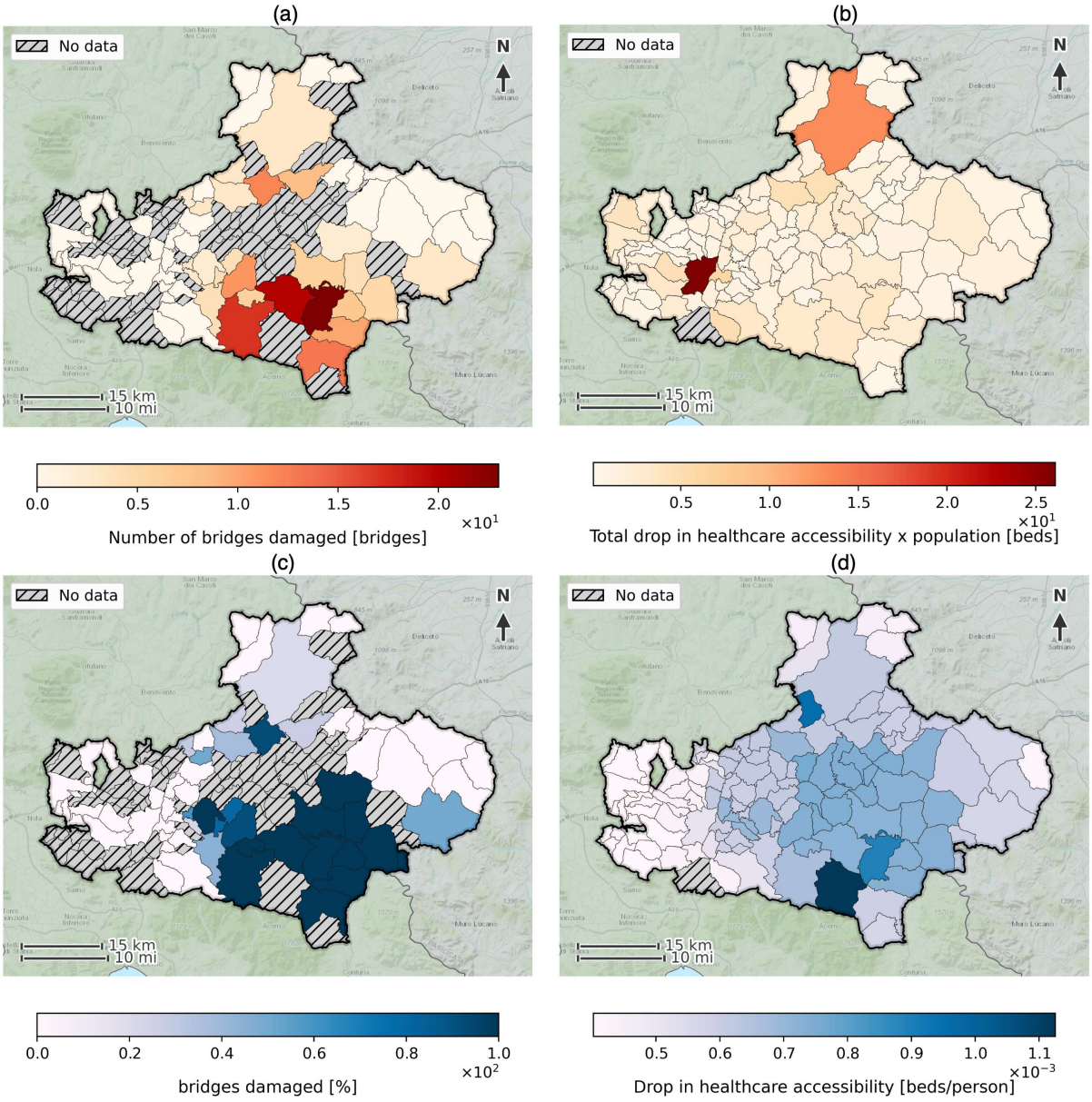

Figure 5: Municipality-level bridge damage (DIM #2) and reduction in healthcare accessibility (DIM #6) following the M_w 6.9 earthquake scenario under the current urban layout. (**a**) Total number of bridges damaged (i.e., whose mean DS is at least 1) within each municipality. (**b**) Population-weighted reduction in healthcare accessibility. (**c**) Percentage of bridges damaged within each municipality. (**d**) Mean reduction in municipality-level healthcare accessibility.

Decision-making on investment prioritisation

Figure 6 presents the decision-making curves obtained when the optimisation is based on total and mean impacts. Both formulations prioritise residential upgrading at low and moderate mitigation targets. Once residential upgrading is nearly complete, bridge retrofitting becomes the main source of further impact reduction, while school upgrading enters only at the highest values of α. The total-impact formulation introduces this diversification slightly earlier, with bridges entering at $\alpha \approx 0.59$ compared with $\alpha \approx 0.68$ under the mean-impact formulation, and schools at $\alpha \approx 0.91$ compared with $\alpha \approx 0.94$; the overall sequencing is nevertheless consistent under both assessment lenses. Hospital upgrading is not selected for any α because only one (out of three) public hospitals is eligible, which makes it less cost-effective than combinations of upgrades across the other asset classes.

Discussion

The Avellino case study demonstrates how integrating system-level societal impacts into seismic risk assessment can reveal mitigation investment priorities that would not emerge from assessments focused on individual assets or direct physical damage. Under both the total- and mean-impact formulations, residential retrofitting delivers the largest initial impact reduction per unit of upgrading effort and is therefore the dominant priority at low and intermediate mitigation targets. Its benefits extend beyond improved structural performance: by reducing residential damage and its long-term implications for recovery, shelter needs and protracted displacement, residential upgrading strengthens both the housing stock and the capacity of affected communities to recover. That this prominence persists under the mean-impact formulation—which removes the influence of differences in the number of exposed assets or infrastructure users across systems—indicates that it does not simply follow from the comparatively large residential inventory, but reflects substantial reductions in normalised societal impacts.

The broader investment sequence is likewise consistent across the two perspectives: the residential stock is upgraded before bridge retrofitting becomes a substantial component of the optimal strategy, and school upgrades emerge only at the highest mitigation targets. The formulations differ not in this ordering but in the thresholds at which investment shifts to additional systems—bridges at $\alpha \approx 0.59$ under the total-impact formulation versus 0.68 under the mean-impact formulation, schools at $\alpha \approx 0.91$ versus 0.94. Priorities are therefore robust to the choice of aggregation perspective, while the point at which cross-system investment becomes preferable is not: the consistently earlier transitions under the total-impact formulation reflect the greater weight aggregate metrics place on consequences accumulated across large numbers of assets and users. The decision-making curves further show that progressively larger upgrading efforts are required to achieve additional impact reductions as α approaches its highest values, reflecting diminishing marginal returns as the most effective intervention opportunities are exhausted.

The increasing importance of bridge retrofitting emphasises why mitigation priorities cannot be understood from direct physical damage alone. As critical components of the road network, bridges influence not only their own functionality but also access to essential services such as healthcare. Their upgrading therefore reduces both the likelihood of bridge

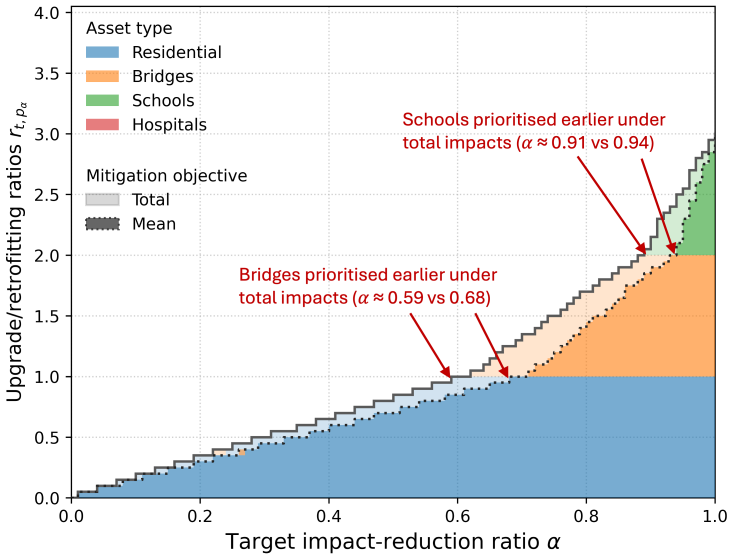

Figure 6: The decision-making curves show the optimal upgrading/retrofitting percentages for each asset type t at a given target impact-reduction ratio α, under both the total-impact and mean-impact benefit formulations.

damage and the wider consequences of network disruption, so that the societal value of an intervention can substantially exceed the avoided damage to the upgraded asset itself. Only one of three hospitals is eligible for upgrading, and the absence of direct hospital upgrades from the optimal strategies should be interpreted in the same context: it does not imply that hospitals are unimportant to seismic resilience, but rather that greater marginal reductions in the combined impacts are achieved elsewhere, including through the transport connectivity that protects healthcare accessibility without upgrading hospital assets directly.

These findings reflect the increasing interconnectedness of infrastructure systems[6,46,58,77], through which disruptions propagate via physical and functional dependencies to affect services beyond the directly damaged assets[78,79]. By linking infrastructure vulnerability to consequences for housing, education, mobility, and healthcare accessibility within a unified optimisation framework, the proposed approach enables asset-level interventions to be evaluated in terms of their broader societal effects. This consequence-oriented perspective also connects seismic mitigation to the wider sustainability agenda, since avoiding damage avoids the repair and reconstruction that follow it, together with the material demands, embodied carbon and diversion of constrained public resources this entails. Prioritising interventions by their system-level consequences therefore provides a basis for risk-informed DRR and urban resilience planning that serves sustainability objectives at the same time.

Several limitations should nevertheless be considered when interpreting these results. First, the case study examines a single hazard type and a specific regional context. Although the general framework can be transferred to other hazards, including floods and wildfires, and to other geographical settings, its application would require hazard, exposure, vulnerability, consequence and intervention models appropriate to those contexts. The specific prioritisation obtained for Avellino province should therefore not be generalised directly to regions with different hazard characteristics, infrastructure configurations, exposure patterns,

or vulnerability profiles. Aleatory variability in ground shaking, residential building impeding factor delay and repair time, and selection of upgraded assets is explicitly sampled, whereas epistemic uncertainty in exposure, fragility and consequence models, accessibility assumptions, and DIM weights is not propagated through the portfolio optimisation. Future applications could incorporate probabilistic representations of these uncertainties and evaluate whether the resulting intervention priorities remain robust across alternative model assumptions and hazard realisations.

Second, upgrading effort is represented through upgrading ratios rather than financial costs[80,81]. The optimisation minimises the sum of the proportions of assets upgraded across infrastructure typologies rather than the monetary expenditure required to implement those interventions. This provides a transparent proxy for mitigation effort and is consistent with approaches adopted in previous studies[40,82], but it does not capture potentially substantial differences in retrofitting costs among infrastructure systems or individual assets[83,84]. Accordingly, terms such as 'efficient' or 'preferable' refer here to performance relative to the adopted upgrading-ratio measure and should not be interpreted as monetary cost-effectiveness. Incorporating asset-specific intervention costs would allow future applications to represent budget constraints more realistically and to support explicit cost–benefit analysis.

Finally, structural upgrading is considered here as the mitigation strategy to demonstrate the framework. In practice, DRR policies can combine structural interventions with land-use planning[85,86], earthquake early-warning systems[87,88], emergency-response planning[89,90], preparedness and risk-communication programmes[17,91], and financial risk-transfer mechanisms[52,92]. Extending the optimisation to represent combinations of structural and non-structural measures, together with their costs, uncertainties, and implementation constraints, would provide a more complete representation of real-world DRR decision-making.

The practical implication of the Avellino case study is that mitigation strategies should be evaluated at the level of ambition actually being targeted rather than at a single nominal optimum, since the preferred allocation across infrastructure sectors shifts systematically as targets become more demanding. Doing so allows limited resources to be directed towards interventions whose benefits propagate through infrastructure interdependencies, protecting access to essential services given constrained economic and environmental resources. This is precisely the capacity on which long-term urban resilience and sustainability depend, and advancing it is central to the objectives of the Sendai Framework and to SDG 9 and SDG 11.

Methods

Exposure modelling

We characterise exposure along two dimensions: physical asset exposure, comprising the built assets susceptible to earthquake damage, and population exposure, comprising the people associated with these assets whose livelihood and access to essential services may be affected. Here, we summarise the datasets and modelling assumptions used to represent both dimensions; further details, including the number of buildings and population for each municipality, the number of students for each school, and the number of beds for each hospital, are provided in the Supplementary Information.

Physical asset exposure

We consider 114,031 reinforced concrete (RC) and unreinforced masonry (URM) residential buildings (which account for 90.54% of the entire building stock of the Avellino province), 512 schools, three public hospitals (that are part of the emergency network identified by the Italian Ministry of Health[93,94]), and 513 bridges. The residential building inventory is obtained by disaggregating 2011 Italian National Institute of Statistics (ISTAT) census data[95] to estimate the number of buildings belonging to each typology within each census tract (*Sezione di Censimento*, SEZ), following an Italy-specific building taxonomy[96,97]. The SEZ-level census data provide marginal distributions of residential buildings by lateral load-resisting system (LLRS) material, construction period, and number of storeys (i.e., height class), but not their joint distribution. We reconstruct this distribution using municipality-level ISTAT cross-tabulations of LLRS material, construction period and height class. For each SEZ, iterative proportional fitting is first used to estimate the joint distribution of LLRS material and construction period while preserving the observed SEZ-level totals for both variables. Construction periods are then mapped to the age classes defined by Rosti et al.[96,97], and buildings within each LLRS-material–age combination are distributed among height classes according to municipality-level conditional height distributions. Buildings with LLRS materials other than RC and URM—11,912 buildings (9.46% of the total building stock)—are excluded because their physical vulnerability cannot be reliably characterised given the limited structural information available.

A clarification on terminology is warranted, since the word vulnerability is used in two distinct senses in this work. Following classifications adopted in the Italian National Seismic Risk Platform[98], the construction-era and height classes of Rosti et al.[96,97] are referred to as vulnerability classes: here the term denotes the relative susceptibility to damage of a building typology, inherited from its design code level and structural configuration, and carries no quantitative meaning on its own. Separately, and consistently with the wider risk-assessment literature[67], we assign to each asset a fragility model and a consequence model, which is ultimately equivalent to a vulnerability model.

Specifically, the resulting residential building exposure follows the taxonomy proposed by Rosti et al.[96,97]. RC buildings are classified into three construction-era classes (1946–1970, 1971–1980 and post-1980, corresponding to structural designs considering only gravity loads, low seismic design code, moderate seismic design code[99], respectively) and three height classes: low-rise (LR; 1–2 storeys), mid-rise (MR; 3 storeys) and high-rise (HR; 4 or more storeys). URM buildings are classified into six construction-era classes (pre-1919, 1919–1945, 1946–1961, 1962–1971, 1972–1981 and post-1981, reflecting URM-specific building code evolution[97]) and two height classes: low-rise (LR; 1–2 storeys) and mid-rise (MR; 3 or more storeys). In both cases the construction-era class acts as a proxy for the code level and hence for the seismic vulnerability. Each typology is identified by its LLRS material, construction-era class and height class (for example, RC+1971–1980+MR).

Table 2 presents the number of residential buildings belonging to each of the 21 typologies across all SEZs in the Avellino province.

Information on schools and hospitals is obtained from the EUCLIDE (EUCentre for Loss Impact and Damage Evaluation) web platform, developed by the European Centre for Training and Research in Earthquake Engineering (EUCentre) for earthquake loss and impact

Table 2: Number of residential buildings for each typology in the Avellino province.

Typology	Count	Typology	Count
RC+>1980+LR	20,574	RC+1971-1980+MR	2,622
URM+>1981+LR	15,650	URM+1962-71+MR	2,080
RC+>1980+MR	12,375	URM+1972-81+MR	1,925
URM+1962-71+LR	11,206	URM+<1919+MR	1,873
URM+1972-81+LR	9,511	RC+1946-1970+MR	1,770
URM+1946-61+LR	7,605	URM+1946-61+MR	1,492
URM+<1919+LR	6,511	URM+1919-1945+MR	1,345
URM+1919-1945+LR	6,208	RC+>1980+HR	739
RC+1971-1980+LR	3,666	RC+1946-1970+HR	543
RC+1946-1970+LR	3,020	RC+1971-1980+HR	382
URM+>1981+MR	2,934		

assessment in Italy[100,101]. For each school and hospital building, EUCLIDE provides its exact location, LLRS material, vulnerability class or seismic design level, and number of storeys. These characteristics together define a unique asset typology. The locations of schools and hospitals are shown in Figure 2. Precise locations are not available for residential buildings, which are instead represented at the SEZ level.

Specifically, five vulnerability classes are defined for school and hospital buildings following the classification adopted in EUCLIDE[100,101]: Class A: high-vulnerability URM buildings; Class B: medium-vulnerability URM buildings; Class C: low-vulnerability URM buildings; Class D: RC frame buildings without earthquake-resistant design; Class E–F: RC frame buildings with earthquake-resistant design. Such vulnerability classification is based on the LLRS material and either the vulnerability level of masonry buildings or the seismic design level of RC buildings. RC buildings have frames as their LLRS, whereas URM buildings have walls as their LLRS. For URM buildings, the vulnerability level broadly reflects the construction era and, consequently, the applicable code level[102]. High-vulnerability buildings were most likely constructed before 1900, medium-vulnerability buildings between 1900 and 1971, and low-vulnerability buildings after 1971. Buildings within each vulnerability class are further classified into four height classes: one storey, two storeys, three storeys, and four or more storeys.

The bridge exposure inventory comprises 513 individually geolocated assets characterised by EUCentre as part of the MARADONA (multi-hazard risk maps for optimal and multi-objective intervention strategies) project. Unlike residential, school and hospital buildings, bridges are not grouped into predefined structural typologies. Instead, each bridge is represented using the asset-specific structural characteristics recorded in the inventory, which are subsequently used to assign the corresponding fragility model. The road network of Avellino province (see Figure 2) is extracted from OpenStreetMap using the Python package OSMnx[103] and represented as a graph, in which nodes correspond to road intersections, and edges represent road segments. Each bridge is linked to the nearest segment within the road network, such that bridge disruption affects network connectivity.

Population exposure

In addition to physical assets, we characterise the population exposure associated with them. This comprises the residents of residential buildings, including 216,270 households and 385,681 individuals; 58,725 students attending school buildings; and the capacity of hospital buildings, represented by 808 beds. Information on households and individuals is obtained from the 2011 Italian Census[104] and allocated to residential building typologies at the SEZ-level in proportion to storey-weighted building counts.

For school buildings, publicly available student enrolment data are obtained from an official report by Regional School Office–Campania[105]. These data include school type, detailed address and number of students, and are spatially matched to the georeferenced school-building dataset provided by EUCentre[106] to derive the spatial distribution of students. Similarly, information on hospital beds is obtained from a report on the hospital network of the Campania region[107]. The reported hospital type, detailed address and number of beds are spatially linked to the georeferenced dataset of hospital buildings registered in the National Emergency Response System as part of the EUCLIDE platform.

Seismic Hazard Modelling

We consider two deterministic earthquake scenarios with M_w of 5.0 and 6.9 occurring within Avellino Province. The more frequent M_w 5.0 scenario is represented as a point source, whereas the devastating M_w 6.9 scenario adopts the rupture geometry of the 1980 Irpinia earthquake mainshock obtained from the Global Earthquake Impact Database[108]. The corresponding source representations are shown in Figure 2. A scenario-based approach is adopted because it enables effective communication of potential earthquake consequences and supports risk-informed decision-making by non-technical policymakers, who may not have a strong intuitive understanding of probabilistic hazard occurrences and impact metrics[109,110].

For each scenario, we use the Italy-specific empirical ground-motion model (GMM) developed by Huang and Galasso[111] to generate 1,000 realisations of spatially correlated peak ground acceleration (PGA). PGA is simulated at the centroids of the SEZs and at the locations of individual assets, including schools, hospitals and bridges. The V_{S30} values (the average shear wave velocity of the upper 30 m, commonly used in GMMs to account for the seismic soil behaviour[112]) are obtained from a large-scale map of V_{S30} for Italy with a spatial resolution of 50×50 m[113] and assigned to each SEZ centroid and asset location.

Figure 7 shows the median PGA across the 1,000 simulated realisations, both at the SEZ centroids of Avellino province (panels a and b) and at the locations of schools, hospitals and bridges (panels c and d), for the M_w 5.0 and M_w 6.9 scenarios respectively. The M_w 5.0 scenario produces median PGA of roughly 0.10–0.15 g near the epicentre, decaying below 0.05 g towards the northern and western areas of the province. The PGA associated with the M_w 6.9 scenario is four to five times more severe, reaching about 0.5 g in the SEZs overlying the rupture and remaining above 0.15 g even in the far north-west, with the highest values elongated along the strike of the rupture.

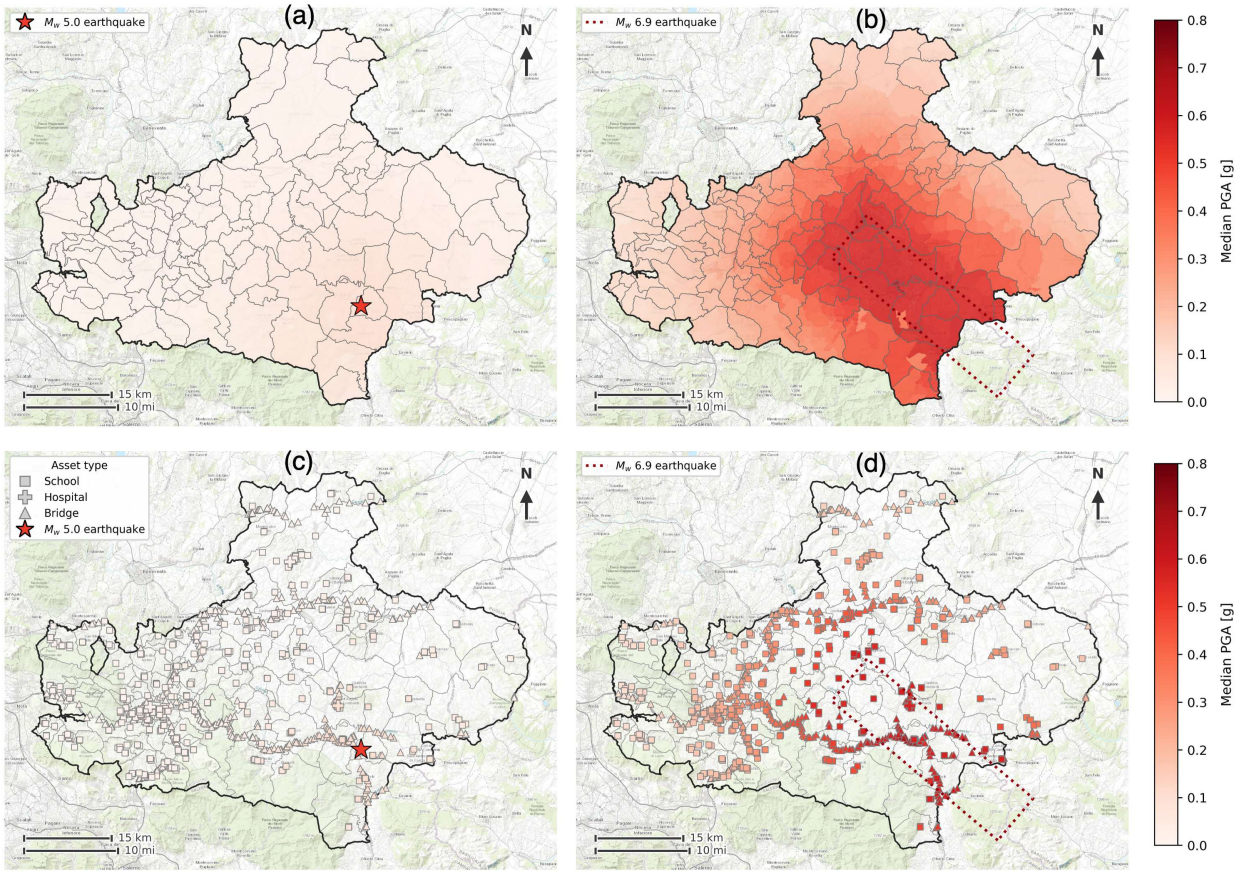

Figure 7: Spatial distribution of median PGA values for the M_w 5.0 and M_w 6.9 earthquake scenarios in Avellino Province. (**a**, **b**) Median PGA values at the centroids of census sections (SEZs) for the M_w 5.0 and M_w 6.9 scenarios, respectively. (**c**, **d**) Median PGA values at the locations of schools, hospitals, and bridges for the M_w 5.0 and M_w 6.9 scenarios, respectively.

Physical Infrastructure Impact

We assess physical damage to residential buildings, schools, hospitals and bridges in terms of discrete DSs, using fragility models assigned according to building typology or derived analytically for individual bridges. Conditioned on each PGA realisation, the most likely DS is computed for each asset or residential typology.

Residential buildings

We characterise the physical impact on residential buildings using the fragility models developed by Rosti et al. for representative Italian RC frame[96] and URM[97] buildings. Each of the 21 residential building typologies listed in Table 2 is assigned a unique set of fragility models. The parameters defining fragility models for the RC frame and URM buildings are reported in Rosti et al.[96] and Rosti et al.[97], respectively.

Following the implementation adopted in the EUCLIDE platform[101] and the development of fragility models for Italian RC frame and URM buildings[96,97], we consider five building DSs of increasing severity (see Table 3): 1-slight damage, representing minor and localised damage with little effect on building stability; 2-moderate damage, representing more widespread but repairable damage; 3-extensive damage, representing substantial damage that considerably impairs building safety and functionality; 4-complete damage, representing very heavy damage involving major failure of building components and likely loss of use; and 5-collapse, representing partial or total building collapse. For each building typology, the probabilities of reaching or exceeding these DSs are evaluated using the corresponding fragility models and simulated PGA values.

Table 3: Damage states defined for different types of physical assets in Avellino province.

Physical asset	**Damage states and descriptions**
Buildings	(1) Slight damage—minor and localised damage with little effect on building stability (2) Moderate damage—widespread but repairable damage (3) Extensive damage—substantial damage that considerably impairs building safety and functionality (4) Complete damage—very heavy damage involving major failure of building components and likely loss of use (5) Collapse—partial or total collapse of the building
Bridges	(1) Damage—can no longer be used without retrofit interventions, although it remains stable from a structural safety perspective (2) Collapse—no longer safe to carry the design vertical loads

School and hospital buildings

We characterise the physical impact on school and hospital buildings using the fragility models assigned according to vulnerability class and height class. Each combination of vulnerability class and number of storeys defines a unique typology corresponding to a predefined set of seismic fragility models embedded within the EUCLIDE platform[101].

Bridges

For bridges, fragility models are not assigned according to predefined structural typologies. Instead, asset-specific bridge fragility functions are provided directly by EUCentre for each individual bridge asset in the study area, based on detailed structural characterisation and numerical analyses[114,115]. These fragility functions were developed within a national framework for large-scale seismic vulnerability assessment of Italian road bridges, in which bridge inventories are classified according to their structural characteristics and appropriate analytical models are adopted to derive asset-level fragility relationships. The derivation accounts for the governing structural failure mechanisms, including failure of piers, abutments, bearings and deck connections for girder bridges, as well as global and local collapse mechanisms for arch bridges, while explicitly incorporating uncertainties in structural properties and seismic demand through Monte Carlo simulation.

Following the implementation in the EUCLIDE platform[101], two bridge DSs are considered. The first, 1-damage, corresponds to exceedance of the Usability Limit State, at which the bridge remains structurally stable but cannot be used without repairs, resulting in a loss of functionality. The second, 2-collapse, corresponds to exceedance of the Collapse Limit State, at which the bridge is no longer safe to carry the design vertical loads. For each bridge, the probabilities of exceeding these DSs are evaluated using the bridge-specific fragility functions and the simulated PGA values.

Mitigation Strategies

A total of 194,481 mitigation strategies are evaluated, consisting of one baseline policy (i.e., the current, unmodified urban layout) and 194,480 compound mitigation strategies. The mitigation strategies represent all possible combinations of upgrade levels (0%, 5%, 10%, ..., 100%) applied to four asset classes—residential buildings, bridges, schools and hospitals—resulting in $21^4 = 194{,}481$ possible configurations. A total of 80,343 residential buildings, 493 bridges, 31 schools and one hospital (consisting of 9 individual buildings) are identified as eligible for upgrading. Eligibility is determined on the basis of the seismic code level associated with each asset (or residential typology), with only assets not already designed to the highest available code level considered eligible. For each mitigation strategy, the prescribed upgrading ratio for each asset class determines the proportion of eligible assets to be upgraded. Because a given upgrading ratio does not uniquely identify which individual assets receive the intervention, eligible assets are randomly selected within each asset class. Twenty independent upgrade-allocation realisations are generated with replacement for each mitigation strategy, each representing a potentially different selection of assets satisfying the same prescribed upgrading ratios. The earthquake impact assessment is repeated for each allocation realisation, and the resulting impact metrics are averaged across the 20 realisations before the mitigation strategy is evaluated in the decision-making analysis. This procedure reduces the influence of any particular random allocation of upgraded assets on the estimated performance of a mitigation strategy. Upgraded assets are assumed to achieve the highest attainable seismic design standard for their respective asset class. This improvement is represented in the analyses through alternative fragility models that reflect the reduced physical vulnerability of upgraded assets.

For residential buildings, each eligible typology is upgraded to the most recent construction-

era class available for the same LLRS material and height class (i.e. post-1980 for RC and post-1981 for URM), the number of storeys and the LLRS material remaining unchanged. For non-residential buildings (schools and hospitals), high- and medium-vulnerability URM buildings (i.e., vulnerability classes A and B) are upgraded to low-vulnerability URM buildings (i.e., vulnerability class C), while RC frame buildings without earthquake-resistant design are upgraded to RC frame buildings with earthquake-resistant design. Hospital buildings are upgraded from vulnerability class D to class E-F, with the number of storeys unchanged. Bridges are upgraded to the strongest typology available within the existing portfolio in Avellino.

Although upgrades are implemented as simple changes in fragility class, each upgrade level corresponds to well-established retrofit interventions in engineering practice. For RC buildings, common measures include column and beam jacketing (concrete or steel) to increase strength and confinement/ductility; externally bonded Fibre Reinforced Polymer (FRP) or Textile Reinforced Mortar (TRM) for shear and flexural strengthening; addition of RC shear walls or infill strengthening to increase lateral stiffness; and, where feasible, base isolation or energy-dissipation devices to reduce seismic demand[116–118]. For URM buildings, representative interventions include improved wall-to-floor anchorage and diaphragm strengthening, installation of ring beams or RC belts, through-bolts and steel ties to improve integrity, and surface or internal strengthening (TRM/FRP overlays, grout injection) to increase in-plane and out-of-plane capacity[119,120]. For bridges, standard upgrades include bearing replacement or retrofit, column confinement or jacketing, deck-to-substructure connection strengthening, and installation of isolation bearings or dampers[121,122]. Each class of intervention reduces vulnerability by increasing capacity, ductility, or continuity and thereby justifies the alternative fragility curves used for the higher upgrade levels. These interventions are routinely implemented under national retrofit programmes and incentive schemes and therefore represent feasible, policy-relevant pathways from the modelled upgrade scenarios to on-the-ground action[35,62].

Social Impact

Residential building recovery

Residential building recovery time (DIM #1) is defined as the sum of building repair time and impeding-factor (IF) delays, which capture additional recovery time arising from administrative and financial bottlenecks and other resource constraints[123]. Using the DS calculations, we quantify building repair time using seismic consequence models developed for Italian archetype RC frame buildings[124]. We adopt the models for three-storey, low-code buildings—constructed before the introduction of modern seismic design codes in Italy—as these most closely represent the majority of the residential building portfolio in Avellino province. The corresponding repair-time distributions (expressed as ratios of the replacement time) are obtained from Aljawhari et al.[124]. We assume a replacement time of 198 days, consistent with observations from contractors following the 2009 L'Aquila earthquake[125].

IF delays are sampled from modified lognormal distributions obtained from Tool for Recovery Estimation And Downtime Simulation[126] and empirically calibrated using recovery data from the 2009 L'Aquila earthquake[125]. The resulting Italy-specific distributions of the individual earthquake IF delays are provided in the Supplementary Information. Recall

that for each PGA realisation, one most likely DS is computed for each residential building typology. Conditional on this DS, 100 samples of building repair time and each individual IF delay are generated, producing 100 recovery-time samples for each SEZ, PGA realisation and residential building typology. Each sampled recovery time is then multiplied by the number of residential buildings belonging to the corresponding typology within the SEZ. These values are aggregated across the SEZs within each municipality to obtain the total and mean recovery times for residential buildings at the municipality level.

Bridge damage

Bridge DS (DIM #2) estimates are obtained directly from the Physical Infrastructure Impact assessment and aggregated across bridges within each municipality to calculate the corresponding total and mean values.

Shelter needs and population displacement

We characterise the peak population requiring immediate shelter assistance during the first month (DIM #3) and the population experiencing protracted displacement lasting over six months (DIM #4), following Paul et al.[127]. For each damage realisation, H denotes the expected number of residents rendered homeless within the municipality, calculated by aggregating the population associated with residential buildings reaching a mean DS ≥ 3 (i.e., extensive damage or worse). The number of sheltered people, N_{sh}, is estimated as

$$\ln\left(N_{\mathrm{sh}}\right) = c_0 + c_1 h^* + c_2 \mathbb{1}(h > 5.7) + c_3 \mathbb{1}(I > 0.7) + c_4 \mathbb{1}(P > 0.06) + c_5 \mathbb{1}(A > 0.67), \quad (8)$$

whereas the number of people experiencing protracted displacement, N_{pr}, is estimated as

$$\ln\left(N_{\mathrm{pr}}\right) = c_0 + c_1 h^* + c_2 P^* + c_3 (hP)^*, \quad (9)$$

where $h = \ln(H)$. Here, I is the national income index, a subcomponent of the Human Development Index describing a country's level of development[128]; P is the national Palma ratio, a measure of income inequality[129]; A is the national age dependency ratio, taken from the World Bank World Development Indicators[130]; and $\mathbb{1}(\cdot)$ is an indicator function equal to one when the stated condition is satisfied and zero otherwise.

The starred quantities in Equations 8 and 9 denote predictors truncated to the bounds which reflect the range of the data on which the underlying regressions were trained: $h^* = \min\left(h,\, 14.62\right)$, $P^* = \min\left(\max\left(P,\, 0.02\right),\, 0.15\right)$, and $(hP)^* = \min\left(\max\left(hP,\, 0.09\right),\, 1.30\right)$. Both models are assigned $N_{\mathrm{sh}} = N_{\mathrm{pr}} = 0$ below the lower bound on h, that is, whenever $h < 4.45$ ($H \leq 86$ residents).

We adopt Italy-specific values of $I = 0.941$, $P = 0.038$, and $A = 0.58$, which are held constant across the study area, together with the coefficient estimates from Paul et al.[127]. Specifically, the coefficients for sheltered displacement are $c_0 = -2.264$, $c_1 = 0.839$, $c_2 = 2.898$, $c_3 = 0.623$, $c_4 = -1.068$, and $c_5 = 1.120$, whereas those for protracted displacement are $c_0 = -10.331$, $c_1 = 1.881$, $c_2 = 133.317$, and $c_3 = -13.998$. The models are reported with pooled held-out residual standard deviations in log space of $\sigma_{\mathrm{sh}} = 1.642$ and $\sigma_{\mathrm{pr}} = 1.808$. Because the present study compares mitigation policies rather than forecasting absolute displacement, we evaluate both models at their median prediction and do not propagate this residual uncertainty; displacement estimates are therefore a deterministic function of

H, and differences between policies reflect changes in damage alone. The equations are applied independently to each municipality using its corresponding value of H. The resulting municipality-level population estimates are divided by the corresponding total municipal populations to derive mean impacts, expressed as percentages of the population.

Students' loss of access to schools

We characterise the number of students losing access to in-person education (DIM #5) by combining school-level DS estimates with student enrolment data. For each municipality, we aggregate the enrolment of schools reaching a mean DS ≥ 2 (i.e., moderate damage or worse). The resulting municipality-level counts of affected students are divided by the corresponding total student enrolment to derive mean impacts, expressed as percentages of students affected.

Impact on healthcare accessibility

DIM #6 quantifies the reduction in municipality-level healthcare accessibility caused by earthquake-induced disruptions to the transportation network and earthquake-induced damage to hospitals. We do not model injuries or casualties. Instead, we evaluate the extent to which the general population can continue to reach functioning hospitals following an earthquake. This deliberate scope emphasises inequities in geographic access, recognising that differences in travel times/distances and the number of reachable facilities can reveal spatially underserved populations and inform targeted infrastructure investment[131]. The municipal centroids and hospital locations are assigned to their nearest nodes in the road network of Avellino province, and the shortest paths are calculated between each pair of centroids and hospitals using the Dijkstra algorithm[132,133]. Post-earthquake accessibility is degraded through two mechanisms. First, bridges expected to experience damage (i.e., mean DS ≥ 1) are assumed to become non-functional, and the corresponding edges are removed from the network to simulate post-earthquake conditions; a hospital is considered unreachable only if all possible routes (i.e., edges) connecting a municipality to that hospital are disrupted due to bridge damage. Second, hospitals expected to experience at least slight damage are treated as non-functional (i.e., mean DS ≥ 1, reduced from 2 for school and residential buildings to reflect that hospital can be rendered non-operational due to slight, non-structural damage to the utilities and equipment[134]) and removed from the set of available healthcare destinations, i.e., their capacity is excluded from the accessibility computation. The shortest-path distances are then recomputed on the modified network and used within a Floating Catchment Area (FCA) approach to calculate a municipal-level healthcare accessibility index, following Wan et al.[135], McGrail and Humphreys[136], Shang et al.[137]. The FCA method is a spatial accessibility approach that quantifies access to services by simultaneously accounting for service capacity (i.e., the number of hospital beds), population demand (i.e., the population potentially served) and travel distance between the municipal centroids and hospitals. The drop in accessibility for each municipality is defined as the difference between the pre-earthquake accessibility index and the post-earthquake accessibility index. Since this DIM focuses only on reductions in accessibility, positive changes (i.e., an increased accessibility after the earthquake) are capped at zero. The accessibility

index A_j for municipality j is defined as:

$$A_j = \sum_{h \in \{d_{j,h} \le d_0\}} \frac{S_h f(d_{j,h})}{\sum_{q \in \{d_{q,h} \le d_0\}} D_q f(d_{q,h})} \tag{10}$$

where D_q is the population of demand municipality q satisfying $d_{q,h} \le d_0$, $d_{j,h}$ is the distance between municipality j and hospital h, and d_0 is the threshold travel distance representing the maximum distance people are willing to travel to access healthcare services. S_h denotes the capacity of hospital h (measured by the number of hospital beds), and $f(d_{j,h})$ is a distance-decay function that weights supply and demand to reflect the decreasing likelihood that people will access hospitals located farther away. In the post-earthquake computation, S_h is set to zero for non-functional hospitals, while the pre-earthquake index is computed on the intact network with all hospitals at full capacity. In this study, we adopt $d_0 = 104$ km, corresponding to the maximum distance between any municipality and hospital within the study area. We adopt a multiple discrete distance-decay function consistent with Shang et al.[137] and Luo et al.[138]. The distance-decay function $f(d_{j,h})$ is defined as:

$$f(d_{j,h}) = \begin{cases} 1.00 & \text{if } d_{j,h} < 0.2 \times d_0 \\ 0.80 & \text{if } 0.2 \times d_0 \le d_{j,h} < 0.4 \times d_0 \\ 0.55 & \text{if } 0.4 \times d_0 \le d_{j,h} < 0.8 \times d_0 \\ 0.15 & \text{if } 0.8 \times d_0 \le d_{j,h} < d_0 \\ 0 & \text{if } d_{j,h} \ge d_0 \end{cases} \tag{11}$$

CRediT authorship contribution statement

C.W.: Writing – original draft, Visualization, Software, Methodology, Investigation, Data curation, Formal analysis, Conceptualization. **A.C.**: Writing – review & editing, Methodology, Investigation, Project administration, Supervision, Data curation, Conceptualization. **N.C.**: Writing – review & editing, Methodology, Investigation, Project administration, Supervision, Funding acquisition, Conceptualization. **C.G.**: Writing – review & editing, Methodology, Investigation, Project administration, Supervision, Funding acquisition, Conceptualization. **A.O.**: Funding acquisition, Conceptualization.

Acknowledgements

We thank Dr. Marta Faravelli and the European Centre for Training and Research in Earthquake Engineering (EUCentre) for providing exposure information on schools, hospitals, and bridges, and associated fragility models. This project has received funding from Next-GenerationEU, within the research project "multi-Risk sciEnce for resilienT commUnities undeR a changiNg climate (RETURN)" (Codice progetto MUR: PE00000005—CUP LEAD PARTNER: H93C22000610002)

Data Availability Statement

All study data and codes are made available on GitHub at https://github.com/wangcb98/system-level-seismic-impact-assessment, except data that have restricted access according to the providers' requirements.

Competing interests

The authors have no competing interests to declare.

References

[1] T. Elmqvist, E. Andersson, N. Frantzeskaki, T. McPhearson, P. Olsson, O. Gaffney, K. Takeuchi, C. Folke, Sustainability and resilience for transformation in the urban century, Nature sustainability 2 (2019) 267–273.

[2] United Nations Office for Disaster Risk Reduction, Making cities resilient 2030 (MCR2030), https://mcr2030.undrr.org/, 2021. Accessed: 15 August 2026.

[3] T. Elmqvist, G. Barnett, C. Wilkinson, Exploring urban sustainability and resilience, Resilient sustainable cities: A future 1 (2014) 19–28.

[4] C. Wang, F. Nocera, G. Cremen, C. Galasso, V. Manandhar, P. Malla, A bespoke approach to facilitating disaster impact quantification using locally relevant metrics, Natural Hazards Review 27 (2026) 04026002.

[5] S. Loos, M. Macías, M. Karr, L. Peek, Beyond deaths and dollars: Modeling requirements to support equity-focused disaster risk management, Earthquake Spectra 42 (2026) e70009.

[6] T. Logan, B. Rachunok, K. Hardaway, D. Bristow, A. Reilly, D. Johnson, J. Johansson, G. Cremen, J. Boakye, P. Schweizer, Advancing systemic risk assessment for complex, interdependent systems: A research agenda, Risk Analysis 46 (2026) e70243.

[7] S. B. Tan, J. W. McCaughey, S. Loos, N. Maharjan, S. Tadepalli, F. Khan, D. Lallemant, Seen and unseen vulnerabilities: Evaluating recovery from the 2015 nepal earthquake to inform more equitable post-disaster needs assessments, International Journal of Disaster Risk Reduction 115 (2024) 105021.

[8] P. Du, J. Chen, C. Chen, Y. Liu, J. Liu, H. Wang, X. Zhang, Environmental risk evaluation to minimize impacts within the area affected by the wenchuan earthquake, Science of the total environment 419 (2012) 16–24.

[9] M. Caruso, V. Silva, K. Aljawhari, A. M. B. Nafeh, C. Galasso, Unveiling the environmental impact of earthquakes in europe, Nature Communications 17 (2026) 1366.

[10] M. Erdik, K. Şeşetyan, M. Demircioğlu, U. Hancılar, C. Zülfikar, Rapid earthquake loss assessment after damaging earthquakes, Soil Dynamics and Earthquake Engineering 31 (2011) 247–266.

[11] J. Wu, N. Li, S. Hallegatte, P. Shi, A. Hu, X. Liu, Regional indirect economic impact evaluation of the 2008 wenchuan earthquake, Environmental Earth Sciences 65 (2012) 161–172.

[12] H. Sheng, C. He, W. Hu, Intercity economic ties amplify natural disasters spillovers in china, Nature Cities (2026) 1–10.

[13] Y. Ren, D. Ma, W. Wang, Z. Wang, X. Zhao, M. Zhu, Probabilistic assessment of earthquake casualties in residential areas, International Journal of Disaster Risk Reduction 113 (2024) 104902.

[14] C. Wang, G. Cremen, C. Galasso, Should i stay or should i go? leveraging data-driven approaches to explore the effect of various disaster policies on postearthquake household relocation decision-making, Risk Analysis 45 (2025) 2267–2284.

[15] N. Paul, C. Galasso, V. Silva, J. Baker, Population displacement after earthquakes: benchmarking predictions based on housing damage, Seismica 3 (2024).

[16] J. A. León, M. Ordaz, E. Haddad, I. Araújo, Risk caused by the propagation of earthquake losses through the economy, Nature communications 13 (2022) 2908.

[17] R. Costa, C. Wang, J. W. Baker, Incorporating infrastructure damage and household disaster preparedness to assess emergency water needs, in: Lifelines 2022, American Society of Civil Engineers, 2022, pp. 434–442.

[18] T. Tabucchi, R. Davidson, S. Brink, Simulation of post-earthquake water supply system restoration, Civil Engineering and Environmental Systems 27 (2010) 263–279.

[19] C. Wang, R. Costa, J. W. Baker, Simulating post-disaster temporary housing needs for displaced households and out-of-town contractors, Earthquake Spectra (2022) 87552930221112690.

[20] C. Mesta, L. Ceferino, G. Cremen, C. Galasso, Investigating post-earthquake hospital transportation for casualties through agent-based modeling, Earthquake Spectra 41 (2025) 2028–2059.

[21] E. M. Hassan, H. N. Mahmoud, B. R. Ellingwood, Resilience of school systems following severe earthquakes, Earth's future 8 (2020) e2020EF001518.

[22] E. A. Opabola, C. Galasso, Informing disaster-risk management policies for education infrastructure using scenario-based recovery analyses, Nature Communications 15 (2024) 325.

[23] S. Platt, D. Gautam, R. Rupakhety, Speed and quality of recovery after the gorkha earthquake 2015 nepal, International Journal of Disaster Risk Reduction 50 (2020) 101689.

[24] L. He, J. C. Aitchison, K. Hussey, Y. Wei, A. Lo, Accumulation of vulnerabilities in the aftermath of the 2015 nepal earthquake: Household displacement, livelihood changes and recovery challenges, International journal of disaster risk reduction 31 (2018) 68–75.

[25] R. Wilson, E. zu Erbach-Schoenberg, M. Albert, D. Power, S. Tudge, M. Gonzalez, S. Guthrie, H. Chamberlain, C. Brooks, C. Hughes, et al., Rapid and near real-time assessments of population displacement using mobile phone data following disasters: The 2015 nepal earthquake, PLoS currents 8 (2016).

[26] A. Dunant, T. R. Robinson, A. L. Densmore, N. J. Rosser, R. M. Rajbhandari, M. Kincey, S. Li, P. R. Awasthi, M. Van Wyk de Vries, R. Guragain, et al., Impacts from cascading multi-hazards using hypergraphs: a case study from the 2015 gorkha earthquake in nepal, Natural Hazards and Earth System Sciences 25 (2025) 267–285.

[27] H. Chen, Q. Xie, B. Feng, J. Liu, Y. Huang, H. Chen, Seismic performance to emergency centers, communication and hospital facilities subjected to nepal earthquakes, 2015, Journal of Earthquake Engineering 22 (2018) 1537–1568.

[28] Q. Xie, L. Gaohu, H. Chen, C. Xu, B. Feng, Seismic damage to road networks subjected to earthquakes in nepal, 2015, Earthquake Engineering and Engineering Vibration 16 (2017) 649–670.

[29] C. Del Gaudio, S. A. Scala, P. Ricci, G. M. Verderame, Evolution of the seismic vulnerability of masonry buildings based on the damage data from l'aquila 2009 event, Bulletin of Earthquake Engineering 19 (2021) 4435–4470.

[30] H. Kaplan, H. Bilgin, S. Yilmaz, H. Binici, A. Öztas, Structural damages of l'aquila (italy) earthquake, Natural Hazards and Earth System Sciences 10 (2010) 499–507.

[31] M. Dolce, A. Goretti, Building damage assessment after the 2009 abruzzi earthquake, Bulletin of Earthquake Engineering 13 (2015) 2241–2264.

[32] A. J. Imperiale, F. Vanclay, The mechanism of disaster capitalism and the failure to build community resilience: Learning from the 2009 earthquake in l'aquila, italy, Disasters 45 (2021) 555–576.

[33] C. Demartino, G. Quinci, F. Paolacci, Seismic performances of italian schools: A comprehensive overview of risk assessment, retrofitting, and preparedness strategies, International Journal of Disaster Risk Reduction 125 (2025) 105508.

[34] Dipartimento della Protezione Civile, Ritorno a scuola [return to school], Presidenza del Consiglio dei Ministri, Rome, Italy, n.d. https://emergenze.protezionecivile.gov.it/en/seismic/abruzzo-2009-earthquake/schools/.

[35] F. Freddi, C. Galasso, G. Cremen, A. Dall'Asta, L. Di Sarno, A. Giaralis, F. Gutiérrez-Urzúa, C. Málaga-Chuquitaype, S. A. Mitoulis, C. Petrone, et al., Innovations in earthquake risk reduction for resilience: Recent advances and challenges, International Journal of Disaster Risk Reduction 60 (2021) 102267.

[36] Y. Zhang, J. F. Fung, K. J. Johnson, S. Sattar, Review of seismic risk mitigation policies in earthquake-prone countries: lessons for earthquake resilience in the united states, Journal of earthquake engineering 26 (2022) 6208–6235.

[37] Asian Disaster Reduction Center, Sendai framework for disaster risk reduction 2015–2030, United Nations Office for Disaster Risk Reduction: Geneva, Switzerland (2015).

[38] United Nations General Assembly, Transforming our world: The 2030 agenda for sustainable development, United Nations General Assembly, 2015. URL: https://sdgs.un.org/2030agenda.

[39] S. Thacker, D. Adshead, M. Fay, S. Hallegatte, M. Harvey, H. Meller, N. O'Regan, J. Rozenberg, G. Watkins, J. W. Hall, Infrastructure for sustainable development, Nature Sustainability 2 (2019) 324–331.

[40] H. Agrawal, C. Wang, G. Cremen, J. McCloskey, A geophysics-informed pro-poor approach to earthquake risk management, Natural Hazards 121 (2025) 6901–6919.

[41] A. L. Beck, H. Talebiyan, E. J. Cha, L. Duenas-Osorio, Socially-aware retrofit prioritization for electric power networks: integrating network performance and social impact considerations, Sustainable and Resilient Infrastructure 10 (2025) 638–654.

[42] G. Cremen, C. Galasso, J. McCloskey, A simulation-based framework for earthquake risk-informed and people-centered decision making on future urban planning, Earth's Future 10 (2022) e2021EF002388.

[43] G. Cremen, C. Galasso, J. McCloskey, A. Barcena, M. Creed, M. E. Filippi, R. Gentile, L. T. Jenkins, M. Kalaycioglu, E. Y. Mentese, et al., A state-of-the-art decision-support environment for risk-sensitive and pro-poor urban planning and design in tomorrow's cities, International Journal of Disaster Risk Reduction 85 (2023) 103400.

[44] S. Loos, D. Lallemant, F. Khan, J. W. McCaughey, R. Banick, N. Budhathoki, J. W. Baker, A data-driven approach to rapidly estimate recovery potential to go beyond building damage after disasters, Communications Earth & Environment 4 (2023) 40.

[45] L. G. Brunner, D. Skipper, T. M. Logan, Estimating whole-of-event consequences in interdependent infrastructure systems, Reliability Engineering System Safety (2026) 112894.

[46] C. Wang, T. Logan, G. Cremen, Capturing dynamic relationships between built and non-built environments for enriched natural-hazard-related risk assessments, in: AGU Fall Meeting Abstracts, volume 2024, 2024, pp. NH23B–2282.

[47] G. Brutti, G. Cremen, C. Galasso, A disaster risk and resilience analysis framework provides insights for modelling natural hazard-induced human mobility, Communications Earth & Environment 7 (2026) 549.

[48] S. Loreti, E. Ser-Giacomi, A. Zischg, M. Keiler, M. Barthelemy, Local impacts on road networks and access to critical locations during extreme floods, Scientific reports 12 (2022) 1552.

[49] D. Nohrstedt, M. Mazzoleni, C. F. Parker, G. Di Baldassarre, Exposure to natural hazard events unassociated with policy change for improved disaster risk reduction, Nature communications 12 (2021) 193.

[50] G. Cremen, C. Galasso, A decision-making methodology for risk-informed earthquake early warning, Computer-Aided Civil and Infrastructure Engineering 36 (2021) 747–761.

[51] N. Caterino, I. Iervolino, G. Manfredi, E. Cosenza, Comparative analysis of multi-criteria decision-making methods for seismic structural retrofitting, Computer-Aided Civil and Infrastructure Engineering 24 (2009) 432–445.

[52] C. Wang, G. Cremen, R. Gentile, C. Galasso, Design and assessment of pro-poor financial soft policies for expanding cities, International Journal of Disaster Risk Reduction 85 (2023) 103500.

[53] P. Bernard, A. Zollo, The irpinia (italy) 1980 earthquake: detailed analysis of a complex normal faulting, Journal of Geophysical Research: Solid Earth 94 (1989) 1631–1647.

[54] R. Maresca, L. Nardone, G. Pasquale, F. Pinto, F. Bianco, Effects of surface geology on seismic ground motion deduced from ambient-noise measurements in the town of avellino, irpinia region (italy), Pure and applied geophysics 169 (2012) 1173–1188.

[55] V. Imbrenda, C. M. Gómez, M. D'Emilio, C. Samela, L. Salvati, N. Matarazzo, M. Lanfredi, R. Coluzzi, Remote sensing and spatial databases for investigating latent urban-rural dynamics in rural, inland districts of southern italy, Cuadernos de investigación geográfica: Geographical Research Letters 49 (2023) 143–162.

[56] M. Polese, M. Di Ludovico, M. G. d'Aragona, A. Prota, G. Manfredi, Regional vulnerability and risk assessment accounting for local building typologies, International journal of disaster risk reduction 43 (2020) 101400.

[57] UNDRR, The sendai framework terminology on disaster risk reduction "disaster risk management", https://www.undrr.org/terminology/disaster-risk-management, 2017. Accessed 9 March 2026.

[58] F. Nocera, Y. Gamal, C. Wang, G. Cremen, Towards inclusive risk-informed infrastructure development in expanding cities, Communications Engineering 4 (2025) 161.

[59] J.-E. Byun, D. D'Ayala, Urban seismic resilience mapping: a transportation network in istanbul, turkey, Scientific reports 12 (2022) 8188.

[60] UNDRR, The sendai framework terminology on disaster risk reduction "residual risk", https://www.undrr.org/terminology/residual-risk, 2017. Accessed 9 March 2026.

[61] UNISDR, Proposed updated terminology on disaster risk reduction: A technical review, Tech. Rep. No. August (2015).

[62] R. Gentile, S. Pampanin, C. Galasso, A computational framework for selecting the optimal combination of seismic retrofit and insurance coverage, Computer-Aided Civil and Infrastructure Engineering 37 (2022) 956–975.

[63] M. Naoi, M. Seko, K. Sumita, Community rating, cross subsidies and underinsurance: Why so many households in japan do not purchase earthquake insurance, The Journal of Real Estate Finance and Economics 40 (2010) 544–561.

[64] C. N. Nguyen, I. Noy, Comparing earthquake insurance programmes: how would japan and california have fared after the 2010–11 earthquakes in new zealand?, Disasters 44 (2020) 367–389.

[65] T. L. Saaty, Decision making with the analytic hierarchy process, International journal of services sciences 1 (2008) 83–98.

[66] M. Riabacke, M. Danielson, L. Ekenberg, State-of-the-art prescriptive criteria weight elicitation, Advances in Decision Sciences 2012 (2012).

[67] R. Gentile, G. Cremen, C. Galasso, L. T. Jenkins, V. Manandhar, E. Y. Menteşe, R. Guragain, J. McCloskey, Scoring, selecting, and developing physical impact models for multi-hazard risk assessment, International Journal of Disaster Risk Reduction 82 (2022) 103365.

[68] L. T. Jenkins, M. J. Creed, K. Tarbali, M. Muthusamy, R. Š. Trogrlić, J. C. Phillips, C. S. Watson, H. D. Sinclair, C. Galasso, J. McCloskey, Physics-based simulations of multiple natural hazards for risk-sensitive planning and decision making in expanding urban regions, International Journal of Disaster Risk Reduction 84 (2023) 103338.

[69] J. Baker, B. Bradley, P. Stafford, Seismic hazard and risk analysis, Cambridge University Press, 2021.

[70] L. Martins, V. Silva, Development of a fragility and vulnerability model for global seismic risk analyses, Bulletin of Earthquake Engineering 19 (2021) 6719–6745.

[71] F. B. Zhan, et al., Three fastest shortest path algorithms on real road networks: Data structures and procedures, Journal of geographic information and decision analysis 1 (1997) 69–82.

[72] S. Hallegatte, An adaptive regional input-output model and its application to the assessment of the economic cost of katrina, Risk Analysis: An International Journal 28 (2008) 779–799.

[73] K. Jaiswal, D. J. Wald, P. S. Earle, K. A. Porter, M. Hearne, Earthquake casualty models within the usgs prompt assessment of global earthquakes for response (pager) system, in: Human casualties in earthquakes: progress in modelling and mitigation, Springer, 2010, pp. 83–94.

[74] C. Kenny, Disaster risk reduction in developing countries: costs, benefits and institutions, Disasters 36 (2012) 559–588.

[75] M. C. Hoyos, V. Silva, Exploring benefit cost analysis to support earthquake risk mitigation in central america, International Journal of Disaster Risk Reduction 80 (2022) 103162.

[76] G. Vannucci, S. Pondrelli, A. Argnani, A. Morelli, P. Gasperini, E. Boschi, et al., An atlas of mediterranean seismicity, Ann. Geophys 47 (2004) 247–306.

[77] L. Li, A. Chang-Richards, M. Boston, K. Elwood, C. M. Hutt, Post-disaster functional recovery of the built environment: A systematic review and directions for future research, International Journal of Disaster Risk Reduction 95 (2023) 103899.

[78] W. Tong, H. X. Li, F. Nasirzadeh, Y. Ji, F. Yao, R. Zhou, Resilience performance analysis of interdependent infrastructures using fault tree and dynamic bayesian network, Reliability Engineering & System Safety (2026) 112541.

[79] M. Ouyang, Review on modeling and simulation of interdependent critical infrastructure systems, Reliability engineering & System safety 121 (2014) 43–60.

[80] N. Caterino, E. Cosenza, A multi-criteria approach for selecting the seismic retrofit intervention for an existing structure accounting for expected losses and tax incentives in italy, Engineering Structures 174 (2018) 840–850.

[81] A. Dodo, N. Xu, R. A. Davidson, L. K. Nozick, Optimizing regional earthquake mitigation investment strategies, Earthquake Spectra 21 (2005) 305–327.

[82] E. Segal, E. Feitelson, S. Goulden, E. Razin, Y. Rein-Sapir, E. J. Kagan, M. Negev, Residential seismic retrofitting: Contextualizing policy packages to local circumstances, International Journal of Disaster Risk Reduction 81 (2022) 103264.

[83] J. F. Fung, S. Sattar, D. T. Butry, S. L. McCabe, The total costs of seismic retrofits: State of the art, Earthquake Spectra 37 (2021) 2991–3014. URL: https://onlinelibrary.wiley.com/doi/abs/10.1177/87552930211009522. doi:https://doi.org/10.1177/87552930211009522. arXiv:https://onlinelibrary.wiley.com/doi/pdf/10.1177/87552930211009522.

[84] P. Colajanni, J. D'Anna, S. Mancini, L. La Mendola, Tools aiding decision-making for economic resources allocation in seismic retrofitting of residential buildings, International Journal of Disaster Risk Reduction 116 (2025) 105149.

[85] E. Y. Menteşe, G. Cremen, R. Gentile, C. Galasso, M. E. Filippi, J. McCloskey, Future exposure modelling for risk-informed decision making in urban planning, International Journal of Disaster Risk Reduction 90 (2023) 103651.

[86] H. Motamed, M. Ghafory-Ashtiany, K. Amini-Hosseini, B. Mansouri, B. Khazai, Earthquake risk–sensitive model for urban land use planning, Natural Hazards 103 (2020) 87–102.

[87] R. M. Allen, H. Kanamori, The potential for earthquake early warning in southern california, Science 300 (2003) 786–789.

[88] G. Cremen, C. Galasso, Earthquake early warning: Recent advances and perspectives, Earth-Science Reviews 205 (2020) 103184.

[89] L. Ceferino, J. Mitrani-Reiser, A. Kiremidjian, G. Deierlein, C. Bambarén, Effective plans for hospital system response to earthquake emergencies, Nature communications 11 (2020) 4325.

[90] D. A. Alexander, Disaster and emergency planning for preparedness, response, and recovery, Oxford Research Encyclopedia of Natural Hazard Science (2015) 12.

[91] K. W. Hudnut, A. M. Wein, D. A. Cox, K. A. Porter, L. A. Johnson, S. C. Perry, J. L. Bruce, D. LaPointe, The HayWired earthquake scenario—We can outsmart disaster, Technical Report, US Geological Survey, 2018.

[92] K. Goda, F. Wenzel, J. Daniell, Insurance and reinsurance models for earthquake, Encyclopedia of earthquake engineering 10 (2014) 978–3.

[93] M. della Salute, Elenco strutture dell'emergenza ospedaliera, 2019. URL: https://www.salute.gov.it/portale/documentazione/p6_2_8_1_1.jsp?lingua=italiano&id=17.

[94] L. Pinto, S. Bianchini, M. A. Barbieri, G. Cherchi, A. Miceli, M. P. Mirauda, V. S. Russotto, I. Raffaldi, T. Zangardi, D. Perri, et al., The use of pediatric short-stay observation in italy, Italian Journal of Pediatrics 49 (2023) 34.

[95] Italian National Institute of Statistics (ISTAT), 2010 permanent census of population and housing, italy, 2010. URL: https://www.istat.it/en/statistical-themes/censuses/permanent-census-of-population-and-housing/.

[96] A. Rosti, C. Del Gaudio, M. Rota, P. Ricci, M. Di Ludovico, A. Penna, G. Verderame, Empirical fragility curves for italian residential rc buildings, Bulletin of Earthquake Engineering 19 (2021) 3165–3183.

[97] A. Rosti, M. Rota, A. Penna, Empirical fragility curves for italian urm buildings, Bulletin of Earthquake Engineering 19 (2021) 3057–3076.

[98] B. Borzi, M. Onida, M. Faravelli, D. Polli, M. Pagano, D. Quaroni, A. Cantoni, E. Speranza, C. Moroni, Irma platform for the calculation of damages and risks of italian residential buildings, Bulletin of Earthquake Engineering 19 (2021) 3033–3055.

[99] M. Zucconi, L. Sorrentino, M. Di Ludovico, Probabilistic usability-based fragility curves for italian reinforced concrete buildings using census and post-earthquake data, Bulletin of Earthquake Engineering (2026) 1–31.

[100] M. Faravelli, F. Bozzoni, E. Zuccolo, A. Di Meo, D. Quaroni, D. Polli, R. Rodriguez-Plata, L. Martelli, B. Borzi, C. G. Lai, A webgis platform for managing the seismic risk at regional scale: The case study of the emilia-romagna region, Procedia Structural Integrity 44 (2023) 43–50.

[101] B. Borzi, M. Onida, M. Faravelli, M. Pagano, A. Di Meo, D. Quaroni, A. Cantoni, F. Bozzoni, A. Famà, D. Bellotti, et al., The platform euclide–eucentre for loss impact and damage evaluation–main integrated it tools and functionalities, International Journal of Disaster Risk Reduction (2026) 106304.

[102] P. Angeletti, A. Baratta, A. Bernardini, C. Cecotti, A. Cherubini, R. Colozza, L. Decanini, P. Diotallevi, G. Di Pasquale, M. Dolce, et al., Valutazione e riduzione della vulnerabilità sismica degli edifici, con particolare riferimento a quelli strategici per la protezione civile, Rapporto finale, Dipartimento della Protezione Civile-Ufficio Servizio Sismico Nazionale, Roma (2002).

[103] G. Boeing, Osmnx: New methods for acquiring, constructing, analyzing, and visualizing complex street networks, Computers, environment and urban systems 65 (2017) 126–139.

[104] ISTAT, 15th general census of population and housing, Italian National Institute of Statistics, 2011. URL: https://www.istat.it.

[105] Regione Campania, Elenco scuole/plessi: Provincia di avellino, Dipartimento dell'Istruzione, della Ricerca, del Lavoro, delle Politiche Culturali e delle Politiche Sociali, n.d. URL: https://www.mim.gov.it/web/miur-usr-campania/scuole-della-campania, school and school-site registry; accessed 12 August 2026.

[106] S. Cattari, S. Alfano, V. Manfredi, B. Borzi, M. Faravelli, A. Di Meo, F. da Porto, E. Saler, A. Dall'Asta, L. Gioiella, M. Di Ludovico, C. Del Vecchio, C. Del Gaudio, G. Verderame, N. Gattesco, I. Boem, E. Speranza, M. Dolce, S. Lagomarsino, A. Masi, National risk assessment of italian school buildings: The mars project experience, International Journal of Disaster Risk Reduction 113 (2024) 104822. URL: https://www.sciencedirect.com/science/article/pii/S2212420924005843. doi:https://doi.org/10.1016/j.ijdrr.2024.104822.

[107] REGIONE CAMPANIA, Regional plan of hospital network planning pursuant to ministerial decree 70/2015 2016-2018, 2016. URL: https://www.regione.campania.it/assets/documents/dca-n-33-2016-piano-regionale-di-programmazione-rete-ospedaliera.pdf.

[108] Z. Karim Zadeh, V. Silva, C. Yepes-Estrada, M. Caruso, E. So, D. Wald, K. Jaiswal, K. Marano, Development of a global earthquake impact database (geid) for the verification and calibration of loss models, Earthquake Spectra 42 (2026) e70006.

[109] H. Bonstrom, Overcoming public and political challenges for natural hazard risk investment decisions, Master's thesis, University of Colorado at Boulder, 2011.

[110] M. Marti, I. Dallo, P. Roth, A. N. Papadopoulos, S. Zaugg, Illustrating the impact of earthquakes: Evidence-based and user-centered recommendations on how to design earthquake scenarios and rapid impact assessments, International journal of disaster risk reduction 90 (2023) 103674.

[111] C. Huang, C. Galasso, Ground-motion intensity measure correlations observed in italian strong-motion records, Earthquake Engineering & Structural Dynamics 48 (2019) 1634–1660.

[112] B. S. S. C. US, et al., Nehrp guidelines for the seismic rehabilitation of buildings (1997).

[113] F. Mori, A. Mendicelli, M. Moscatelli, G. Romagnoli, E. Peronace, G. Naso, A new vs30 map for italy based on the seismic microzonation dataset, Engineering Geology 275 (2020) 105745.

[114] B. Borzi, A. Famà, C. F. Manzini, P. Morandi, D. Quaroni, Seismic vulnerability assessment of italian road bridges through the definition of fragility curves for bridge taxonomies, 2026. Manuscript under review at the International Journal of Disaster Risk Reduction.

[115] B. Borzi, P. Ceresa, P. Franchin, F. Noto, G. M. Calvi, P. E. Pinto, Seismic vulnerability of the italian roadway bridge stock, Earthquake Spectra 31 (2015) 2137–2161.

[116] K. Aljawhari, R. Gentile, C. Galasso, Beyond direct economic losses: an integrated approach to seismic retrofit considering sustainability and indirect losses, Earthquake Engineering & Structural Dynamics 54 (2025) 1737–1758.

[117] L. N. Koutas, Z. Tetta, D. A. Bournas, T. C. Triantafillou, Strengthening of concrete structures with textile reinforced mortars: State-of-the-art review, Journal of Composites for Construction 23 (2019) 03118001.

[118] V. A. Matsagar, R. Jangid, Base isolation for seismic retrofitting of structures, Practice Periodical on Structural Design and Construction 13 (2008) 175–185.

[119] S. Bhattacharya, S. Nayak, S. C. Dutta, A critical review of retrofitting methods for unreinforced masonry structures, International Journal of Disaster Risk Reduction 7 (2014) 51–67.

[120] A. Wilson, P. J. Quenneville, J. M. Ingham, In-plane orthotropic behavior of timber floor diaphragms in unreinforced masonry buildings, Journal of Structural Engineering 140 (2014) 04013038.

[121] A. Venkittaraman, S. Banerjee, Enhancing resilience of highway bridges through seismic retrofit, Earthquake Engineering & Structural Dynamics 43 (2014) 1173–1191.

[122] T. Wright, R. DesRoches, J. E. Padgett, Bridge seismic retrofitting practices in the central and southeastern united states, Journal of Bridge Engineering 16 (2011) 82–92.

[123] P. Kourehpaz, C. Galasso, C. Molina Hutt, Enhancing resilience through recovery modeling in multi-hazard contexts, Communications Engineering (2026).

[124] K. Aljawhari, R. Gentile, C. Galasso, Simulation-based consequence models of seismic direct loss and repair time for archetype reinforced concrete frames, Soil Dynamics and Earthquake Engineering 172 (2023) 107979.

[125] D. Cardone, A. Flora, M. D. L. Picione, A. Martoccia, Estimating direct and indirect losses due to earthquake damage in residential rc buildings, Soil Dynamics and Earthquake Engineering 126 (2019) 105801.

[126] C. Molina Hutt, T. Vahanvaty, P. Kourehpaz, An analytical framework to assess earthquake-induced downtime and model recovery of buildings, Earthquake Spectra 38 (2022) 1283–1320.

[127] N. Paul, V. Silva, J. Baker, M. Peter, R. Oakes, S. Ponserre, C. Galasso, Predicting population displacement due to earthquakes globally, Nature Communications In press (2026).

[128] U. U. N. D. Programme), Human development report 2020, UNDP (United Nations Development Programme) (2020). URL: http://report2020.archive.s3-website-us-east-1.amazonaws.com/.

[129] World Inequality Database (WID.world), Income inequality: Palma ratio (before tax) – WID, Dataset, 2026. URL: https://archive.ourworldindata.org/20260707-125341/grapher/palma-ratio-wid.html, with major processing by Our World in Data. Original data from the World Inequality Database (WID). Archived on 7 July 2026.

[130] World Bank, Age dependency ratio (% of working-age population), World Development Indicators, 2026. URL: https://data.worldbank.org/indicator/SP.POP.DPND.

[131] K. L. M. Wong, W. Dotse-Gborgbortsi, D. Dwomoh, C. Avoka, S. Shetty, P. Sriram, G. Prasad, M. Kane, M. Young, C. Stanton, A. Banke-Thomas, Inequities in geographic access to emergency obstetric and newborn care in greater accra, Nature Cities (2026). URL: https://doi.org/10.1038/s44284-026-00479-z. doi:10.1038/s44284-026-00479-z.

[132] D. Fan, P. Shi, Improvement of dijkstra's algorithm and its application in route planning, in: 2010 seventh international conference on fuzzy systems and knowledge discovery, volume 4, IEEE, 2010, pp. 1901–1904.

[133] D. Rachmawati, L. Gustin, Analysis of dijkstra's algorithm and a* algorithm in shortest path problem, in: Journal of Physics: Conference Series, volume 1566, IOP Publishing, 2020, p. 012061.

[134] NIST, Community Resilience Planning Guide for Buildings and Infrastructure Systems, Volume II, Technical Report NIST Special Publication 1190, National Institute of Standards and Technology, 2015. doi:10.6028/NIST.SP.1190v2.

[135] N. Wan, B. Zou, T. Sternberg, A three-step floating catchment area method for analyzing spatial access to health services, International Journal of Geographical Information Science 26 (2012) 1073–1089.

[136] M. R. McGrail, J. S. Humphreys, Measuring spatial accessibility to primary health care services: Utilising dynamic catchment sizes, Applied Geography 54 (2014) 182–188.

[137] Q. Shang, X. Guo, J. Li, T. Wang, Post-earthquake health care service accessibility assessment framework and its application in a medium-sized city, Reliability Engineering & System Safety 228 (2022) 108782.

[138] W. Luo, Y. Qi, An enhanced two-step floating catchment area (e2sfca) method for measuring spatial accessibility to primary care physicians, Health & place 15 (2009) 1100–1107.

Supplementary Files

This is a list of supplementary files associated with this preprint. Click to download.

- SupplementaryInformationResilientCities.pdf